The High-Order Shifted Boundary Method and its Analysis

Nabil M. Atallah[a], Claudio Canuto[b], Guglielmo Scovazzi[a,*]

[a] *Department of Civil and Environmental Engineering, Duke University, Durham, North Carolina 27708, USA*
[b] *Dipartimento di Scienze Matematiche, Politecnico di Torino, Corso Duca degli Abruzzi 24, 10129 Torino, Italy*

Abstract

The Shifted Boundary Method (SBM) is an approximate domain method for boundary value problems, in the broader class of unfitted/embedded/immersed methods, that has proven efficient in handling partial differential equation problems with complex geometries. The key feature of the SBM is a *shift* in the location where boundary conditions are applied - from the true to a surrogate boundary - and an appropriate modification (again, a *shift*) of the value of the boundary conditions, in order to reduce the consistency error. This paper presents the high-order version of the method, its mathematical analysis, and numerical experiments. The proposed method retains optimal accuracy for any order of the finite element interpolation spaces despite the surrogate boundary is piecewise linear. As such, the proposed approach bypasses the problematic issue of meshing complex geometries with high-order body-fitted boundary representations, without the need of complex data structures for the integration on cut cells.

Keywords: Shifted Boundary Method; high-order method; Immersed Boundary Method; small cut-cell problem; approximate domain boundaries; unfitted finite element methods.

1. Introduction and overview

The Shifted Boundary Method (SBM) is an approximate domain method for boundary value problems, in the broader class of unfitted/embedded/immersed methods (see, e.g., [9, 14–16, 25, 30, 34, 36, 48, 50, 51, 56]).

In the SBM, the location where boundary conditions are applied is *shifted* from the true boundary to an approximate (surrogate) boundary, and, at the same time, the value of boundary conditions is modified (*shifted*) by means of Taylor expansions, in order to avoid a reduction of the convergence rates of the overall formulation. In fact, if the boundary conditions associated to the true domain are not appropriately modified on the surrogate domain, only first-order convergence is to be expected. The appropriate (modified) boundary conditions are then applied weakly, using a Nitsche strategy. This process yields a method which is simple, robust, accurate and efficient.

The SBM was proposed for the Poisson and Stokes flow problems in [42] and was generalized in [43] to the advection-diffusion and Navier-Stokes equations and in [60] to hyperbolic conservation laws. The benefits of its application in conjunction with reduced order modeling of geometric parameterizations was analyzed in [37–39]. Further rigorous mathematical analysis was pursued in [2–5] for the Poisson, Stokes and linear elasticity equations.

The purpose of this paper is to introduce a high-order version of the SBM, including a sound mathematical analysis. We develop a stability, consistency and convergence analysis for the Poisson and Stokes flow problems with unfitted Dirichlet boundary conditions along with complete L^2-estimates via a duality argument.

One important aspect of the proposed high-order SBM is that it retains optimal rates of convergence even though the surrogate (approximate) boundary is represented by piecewise-linear boundary representations. The Taylor expansions used to correct the solution at the surrogate boundary are effective in maintaining optimal accuracy. The net result is a method that completely bypasses the need for high-order body-fitting of the computational grids, that is

*Corresponding author: Guglielmo Scovazzi

Email addresses: nabil.atallah@duke.edu (Nabil M. Atallah), claudio.canuto@polito.it (Claudio Canuto), guglielmo.scovazzi@duke.edu (Guglielmo Scovazzi)

using high-order polynomials in the representation of element geometry at the boundary. This feature could represent a change in paradigm for high-order methods.

One surprising aspect of the proposed approach is that the geometric representations of boundaries may not even need to be watertight on a fine scale, as long as their resolution is finer than the resolution of the grids utilized in simulations.

From a purely mathematical perspective, the SBM bears some similarities with the boundary approximation method proposed by Bramble, Dupont, and Thomèe [13]. The authors of original SBM work [42] were unaware of this earlier development, which however has also important differences with respect to the SBM. As acknowledged in a later contribution by Bramble and King [12], the method of Bramble, Dupont, and Thomèe [13] was found of impractical implementation, particularly for domains with corners that are ubiquitous in engineering design. On the other hand, the work of Bramble and King [12] requires the assumption that the distance between the surrogate and the true boundary decays as the square of the mesh size, an equally impractical requirement in complex geometry simulations, because it collapses to nearly body-fitting the computational grid to the geometries. In this regard, the SBM does not follow these works and retains the ability to perform efficiently and robustly in geometrically complex engineering simulations [5, 42, 43].

The SBM bears also some intersection with the high-order generalization of the work of Bramble and King presented by Cockburn, Solano and co-authors in [24–26, 48]. However, in those works, the extension of the boundary conditions from the approximate to the true boundary is done by means of the fundamental theorem of calculus rather than Taylor expansions and the strategies to select the paths of integration/extrapolation are different than for the SBM.

Prior to the work of Solano and collaborators, a variety of new embedded/immersed geometry approaches [28, 31, 32, 50] have been proposed to further speed up design and analysis in complex geometry. These approaches started from the realization that the generation of CAD geometrical representations can still be a costly phase in the overall design and analysis process, especially if the geometry is obtained from the pixels/voxels that are the result of two/three-dimensional image reconstruction techniques. Although these methods have borrowed some ideas from extended/enriched/unfitted methods for fracture mechanics [44], they have been designed for a completely different purpose, and for this reason we do not even attempt an account of the developments of the latter, which are peripheral to the discussion here.

Similarly, high-order cutFEM methods have been proposed and analyzed in a number of theoretical papers [7, 19, 40, 41, 47, 49, 52]. High-order extensions of the work in [12, 13] were presented in a series of articles [11, 16, 17, 21–23].

Iso-Geometric Analysis (IGA) [8, 27] was proposed as an alternative paradigm, in which NURBS or T-Spline functions are used to build discrete approximation spaces directly on the CAD representation, somewhat avoiding the costly operation of generating body-fitted grids. However, when the level of complexity of geometric shapes is large, Immerso-Geometric Methods [57] (i.e., immersed methods based on IGA approximation spaces) seem the preferred choice in the IGA community.

More recently, the Method of Universal Meshes was proposed in a series of papers, which also included some extensions to high-order finite element spaces [53–55]. These developments are peripheral to the discussion presented here, since the Method of Universal Meshes is aimed at moving boundary/evolving interface problems and collapses to a body-fitted mesh generation strategy in the case of fixed boundaries.

The SBM falls in the broad category of embedded/immersed methods and addresses some of the long standing problems that have somewhat limited the broader application of such techniques in the engineering practice. Specifically, common embedded strategies for the enforcement of boundary conditions revolve around 1) the use of exact cut-cell geometry representations to construct the solution space and 2) the Nitsche's method [45] for consistent weak boundary enforcement [31]. For body-fitted approaches, employing Nitsche's method does not adversely affect the conditioning of the system matrix. However, in the case of embedded finite elements, due to the arbitrariness of the size of the cut elements, naïve approaches suffer from numerical instabilities and poor matrix conditioning problems. A number of approaches have addressed this issue in recent years [18, 20, 58, 59], but the geometric construction of the partial elements cut by the embedded boundary typically remains a complex and computationally intensive process. Similarly, the construction of appropriately accurate quadrature formulas to integrate the variational equations on cut cell is challenging, and typically relies on the use of sub-triangulations (an approach that somewhat defeats the purpose of immersed methods) or the development of complex quadrature formulas directly in physical space (since there it is not possible to define the parent domain of a cut element of general shape).

The general tradeoff of the SBM is that integration and data management of cut cells is completely avoided, at the expense of variational formulations that include additional terms with respect to the corresponding cutFEMs, Immersogeometric (Immersed IGA) and Finite Cell Methods. We believe that this tradeoff could be advantageous when considering very complex geometries, including the case of non watertight descriptions.

This article is organized as follows: Section 2 introduces the surrogate domain and describes in particular how the exact boundary condition is mapped to the surrogate boundary. The high-order SBM is presented in Section 3 for the Poisson equation, and in Section 4 for the Stokes equations. The coercivity and inf-sup properties of the SBM variational forms are established in Section 5, whereas the continuity properties are established in Section 6. The key Section 7 analyzes the behavior of the Taylor remainder on the surrogate boundary. The consistency and convergence properties of our method are discussed in Section 8 based on Strang's Second Lemma, whereas an enhanced error estimate in the L^2-norm is obtained in Section 9 via an Aubin-Nitsche argument. Finally, representative numerical tests are given in Sect. 10.

2. The shifted boundary conditions

2.1. Notation

Let Ω be a connected open set in $\mathbb{R}^n (n = 2$ or $3)$, with boundary $\Gamma = \partial\Omega$ of class C^{m+1} for some $m \geq 1$. Let $\boldsymbol{n}$ denote the outward-oriented unit normal vector to Γ. Throughout the paper, we will denote by $L^2(\Omega)$ the space of square integrable functions on Ω and by $L^2_0(\Omega)$ the space of square integrable functions with zero mean on Ω (i.e., $q \in L^2_0(\Omega)$ implies $\int_\Omega q = 0$). We will use the Sobolev spaces $H^m(\Omega) = W^{m,2}(\Omega)$ of index of regularity $m \geq 0$ and index of summability 2, equipped with the (scaled) norm

$$\|v\|_{H^m(\Omega)} = \left(\| v \|^2_{L^2(\Omega)} + \sum_{k=1}^{m} \| l(\Omega)^k \boldsymbol{D}^k v \|^2_{L^2(\Omega)} \right)^{1/2} , \tag{1}$$

where $\boldsymbol{D}^k$ is the kth-order spatial derivative operator and $l(A) = \text{meas}_n(A)^{1/n}$ is a characteristic length of the domain A ($n = 2, 3$ indicates the number of spatial dimensions). Note that $H^0(\Omega) = L^2(\Omega)$. As usual, we use a simplified notation for norms and semi-norms, i.e., we set $\| v \|_{m,\Omega} = \| v \|_{H^m(\Omega)}$ and $| v |_{k,\Omega} = \| \boldsymbol{D}^k v \|_{0,\Omega} = \| \boldsymbol{D}^k v \|_{L^2(\Omega)}$. Similarly, we will indicate with $(v, w)_{m,\Omega}$ the $H^m(\Omega)$-inner product and by $(v, w)_{0,\Omega}$ the $L^2(\Omega)$-inner product. We will also use the notation $(v, w)_{0,\Gamma}$ for the $L^2(\Gamma)$-inner product over the boundary Γ of Ω. Furthermore, for two positive scalars A and B, $A \lesssim B$ indicates that there exists a positive constant c, independent of the relevant parameters of the discretization, such that $A \leq c\, B$.

2.2. The true domain, the surrogate domain and maps

In view of the application of the finite element method, we consider a closed domain $\mathscr{D}$ such that $\text{clos}(\Omega) \subseteq \mathscr{D}$ and we introduce a family $\mathscr{T}_h$ of admissible and shape-regular triangulations of $\mathscr{D}$. Then, we restrict each triangulation by selecting those elements that are contained in $\text{clos}(\Omega)$, i.e., we form

$$\tilde{\mathscr{T}}_h := \{T \in \mathscr{T}_h : T \subset \text{clos}(\Omega)\} .$$

This identifies the *surrogate domain*

$$\tilde{\Omega}_h := \text{int}\left(\bigcup_{T \in \tilde{\mathscr{T}}_h} T \right) \subseteq \Omega ,$$

with *surrogate boundary* $\tilde{\Gamma}_h := \partial\tilde{\Omega}_h$ and outward-oriented unit normal vector $\tilde{\boldsymbol{n}}$ to $\tilde{\Gamma}_h$. Obviously, $\tilde{\mathscr{T}}_h$ is an admissible and shape-regular triangulation of $\tilde{\Omega}_h$ (see Figure 1a). As usual, we indicate by h_T (h^i_T, resp.) the circumscribed diameter (inscribed diameter, resp.) of an element $T \in \tilde{\mathscr{T}}_h$ and by h (h^i, resp.) the piecewise constant function in $\tilde{\Omega}_h$ such that $h_{|T} = h_T$ ($h^i_{|T} = h^i_T$, resp.) for all $T \in \tilde{\mathscr{T}}_h$. We introduce the following mesh parameters

$$h_\Gamma := \max_{T \in \tilde{\mathscr{T}}_h : T \cap \tilde{\Gamma}_h \neq \emptyset} h_T , \tag{2a}$$

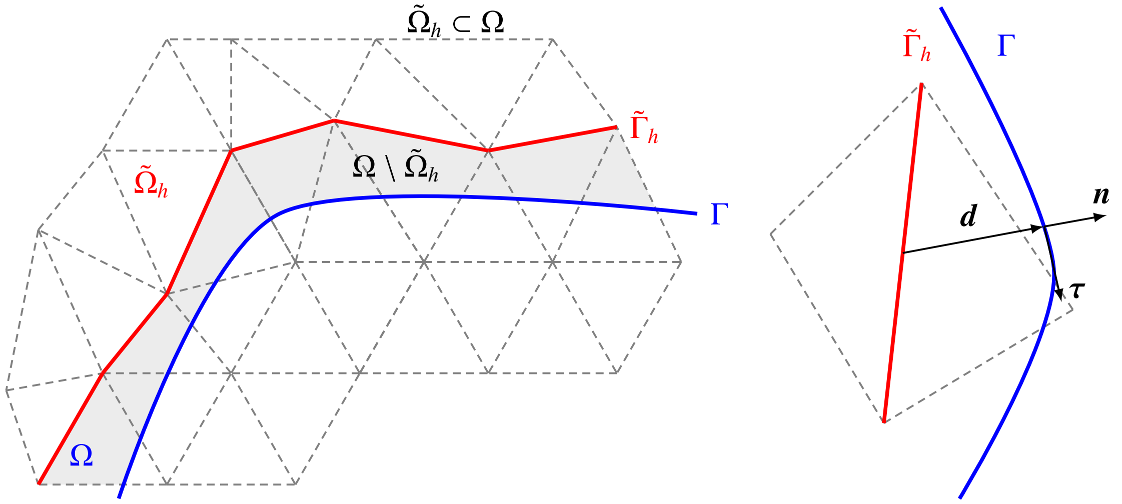

(a) The true domain Ω, the surrogate domain $\tilde{\Omega}_h \subset \Omega$ and their boundaries $\tilde{\Gamma}_h$ and Γ.

(b) The distance vector $\boldsymbol{d}$, the true normal $\boldsymbol{n}$ and the true tangent $\boldsymbol{\tau}$.

Figure 1: The surrogate domain, its boundary, and the distance vector $\boldsymbol{d}$.

$$h_\Omega := \max_{T \in \tilde{\mathscr{T}}_h} h_T \,, \tag{2b}$$

$$h_{\tau,T} := (h_T \, h_T^i)^{1/2} \,, \tag{2c}$$

$$h_{\perp,E} := \frac{\mathrm{meas}_{n_d}(T)}{\mathrm{meas}_{n_d-1}(\tilde{E})} \,, \; \forall \tilde{E} \in \tilde{\Gamma}_h, \;\; T \cap \tilde{E} \neq \emptyset, \;\; T \in \tilde{\mathscr{T}}_h \,. \tag{2d}$$

We assume there exist constants $C_r, \xi_1, \xi_2 \in \mathbb{R}^+$ such that $(1/\sqrt{C_r})\, h \leq h_\tau \leq h$ and $\xi_1 \, h \leq h_\perp \leq \xi_2 \, h$. With a slight abuse of notation, we will assume h, h_τ and $h_\perp$ are interchangeable.

We now select a mapping

$$\boldsymbol{M}_h : \tilde{\Gamma}_h \to \Gamma \,, \tag{3a}$$

$$\tilde{\boldsymbol{x}} \mapsto \boldsymbol{x} \,, \tag{3b}$$

which associates to any point $\tilde{\boldsymbol{x}} \in \tilde{\Gamma}_h$ on the surrogate boundary a point $\boldsymbol{x} = \boldsymbol{M}_h(\tilde{\boldsymbol{x}})$ on the physical boundary Γ. Whenever uniquely defined, the closest-point projection of $\tilde{\boldsymbol{x}}$ upon Γ is a natural choice for $\boldsymbol{x}$, as shown e.g. in Figure 1b, but more sophisticated choices may be locally preferable and we refer to [2] for more details. The mapping (3) can be characterized through a distance vector function $\boldsymbol{d}_{\boldsymbol{M}_h}$ defined by

$$\boldsymbol{d}_{\boldsymbol{M}_h}(\tilde{\boldsymbol{x}}) := \boldsymbol{x} - \tilde{\boldsymbol{x}} = [\boldsymbol{M}_h - \boldsymbol{I}](\tilde{\boldsymbol{x}}) \,. \tag{4}$$

For the sake of simplicity, we will actually set $\boldsymbol{d} = \boldsymbol{d}_{\boldsymbol{M}_h}$, so that we will write $\boldsymbol{x} = \tilde{\boldsymbol{x}} + \boldsymbol{d}(\tilde{\boldsymbol{x}})$. It will be useful to write $\boldsymbol{d} = \|\boldsymbol{d}\|\boldsymbol{\nu}$, where $\boldsymbol{\nu}$ is a unit vector defined on $\tilde{\Gamma}_h$.

In the present work, we assume at least C^2-smoothness of the boundary, in which case $\boldsymbol{M}_h$ is defined with the closest point projection, which implies $\boldsymbol{\nu} = \boldsymbol{n}$. In the case of non smooth boundaries, the mathematical analysis that follows is not applicable and optimal convergence rates cannot be achieved, but other choices for $\boldsymbol{\nu}$ are possible and the analysis will proceed similarly to what is reported in [2]. Note also that, in principle, other strategies are possible to define the map $\boldsymbol{M}_h$ and, correspondingly, the distance vector $\boldsymbol{d}$. Among them, for example, is a level set description of the true boundary, in which $\boldsymbol{d}$ is defined by means of a distance function.

Remark 1. *From the definition of closest-point point projection, it follows that* $\|\boldsymbol{d}(\tilde{\boldsymbol{x}})\| \lesssim h_T$ *for any* $\tilde{\boldsymbol{x}} \in T \cap \tilde{\Gamma}_h$, *whence*

$$\|h^{-1}\boldsymbol{d}\|_{L^\infty(\tilde{\Gamma}_h)} \lesssim 1 \; . \tag{5}$$

2.3. General strategy

In the SBM approach, the governing equations are discretized in $\tilde{\Omega}_h$ rather than in Ω, with the challenge of accurately imposing on $\tilde{\Gamma}_h$ boundary conditions. To this end, we resort to the idea introduced in [42] but instead, perform an mth-order Taylor expansion of the concerned variable at the surrogate boundary in order to *shift* the boundary condition from Γ to $\tilde{\Gamma}_h$.

Let us assume that u is sufficiently smooth in the strip between $\tilde{\Gamma}_h$ and Γ so as to admit a mth-order Taylor expansion pointwise, and let us denote by $\mathscr{D}^i_{\boldsymbol{d}}$ the ith-order directional derivative in the direction of $\boldsymbol{d}$, defined as $\mathscr{D}^i_{\boldsymbol{d}} u = \sum_{\alpha\in\mathbb{N}^n, |\alpha|=i} \frac{i!}{\alpha!}\frac{\partial^i u}{\partial \boldsymbol{x}^\alpha}\boldsymbol{d}^\alpha$. Then, we can write

$$u(\boldsymbol{x}) = u(\tilde{\boldsymbol{x}} + \boldsymbol{d}(\tilde{\boldsymbol{x}})) = u(\tilde{\boldsymbol{x}}) + \sum_{i=1}^{m} \frac{\mathscr{D}^i_{\boldsymbol{d}}\, u(\tilde{\boldsymbol{x}})}{i!} + (R^m(u,\boldsymbol{d}))(\tilde{\boldsymbol{x}}) \, , \tag{6}$$

where the remainder $R^m(u,\boldsymbol{d})$ satisfies $|R^m(u,\boldsymbol{d})| = o(\|\boldsymbol{d}\|^m)$ as $\|\boldsymbol{d}\| \to 0$. Assume now that a Dirichlet condition of the type $u(\boldsymbol{x}) = g(\boldsymbol{x})$ needs to be imposed on the true boundary Γ. Using the map $\boldsymbol{M}_h$, one can extend g from Γ to $\tilde{\Gamma}_h$ as $\bar{g}(\tilde{\boldsymbol{x}}) = g(\boldsymbol{M}_h(\tilde{\boldsymbol{x}}))$. Then, the Taylor expansion can be used to enforce the Dirichlet condition on $\tilde{\Gamma}_h$ rather than Γ, as

$$S^m_h u - \bar{g} + R^m_h u = 0 \, , \tag{7}$$

where we have introduced the boundary operator

$$S^m_h u := u + \sum_{i=1}^{m} \frac{\mathscr{D}^i_{\boldsymbol{d}}\, u}{i!} \tag{8}$$

and $R^m_h u$ is a short-hand notation for the Taylor expansion remainder $R^m(u,\boldsymbol{d})$. Neglecting the remainder $R^m_h u$, we obtain the final expression of the *shifted* boundary condition

$$S^m_h u = \bar{g} \, , \quad \text{on } \tilde{\Gamma}_h \; , \tag{9}$$

which will be weakly enforced on the discretization u_h of u that we are going to introduce. Similarly, for a vector field $\boldsymbol{u}$, we deduce that its trace $\bar{\boldsymbol{g}}$ shifted on $\tilde{\Gamma}_h$ satisfies

$$\boldsymbol{S}^m_h \boldsymbol{u} + \boldsymbol{R}^m_h \boldsymbol{u} = \bar{\boldsymbol{g}} \, , \tag{10}$$

where $\boldsymbol{S}^m_h \boldsymbol{u} := \boldsymbol{u} + \sum_{i=1}^{m} \frac{\mathscr{D}^i_{\boldsymbol{d}}\, \boldsymbol{u}}{i!}$ on $\tilde{\Gamma}_h$ and $\boldsymbol{R}^m_h \boldsymbol{u}$ is the Taylor expansion remainder of $\boldsymbol{u}$ on $\tilde{\Gamma}_h$. Again, neglecting the the remainder $\boldsymbol{R}^m_h \boldsymbol{u}$, we obtain the *shifted* vector boundary condition

$$\boldsymbol{S}^m_h \boldsymbol{u} = \bar{\boldsymbol{g}} \, , \quad \text{on } \tilde{\Gamma}_h \; . \tag{11}$$

In what follows, whenever it does not cause confusion, the bar symbol will be removed from the extended quantities, and we would write g and $\boldsymbol{g}$ in place of $\bar{g}$ and $\bar{\boldsymbol{g}}$, respectively. Before proceeding with the analysis of the Poisson and Stokes problems using the Shifted Boundary Method, we make the following

Assumption 1. *The Neumann boundary is body-fitted, that is* $\Gamma_N \subset \tilde{\Gamma}_h$.

According to this assumption, the surrogate boundary where shifted Dirichlet conditions are enforced is $\tilde{\Gamma}_{D,h} := \tilde{\Gamma}_h \setminus \Gamma_N$.

Remark 2. *Assumption 1 is made for the mathematical proofs of stability and convergence, but is not a restrictive assumption in numerical computations. We refer the interested reader to [5], where Neumann boundaries are "shifted"* *using a mixed variational formulation. In particular, shifting the Neumann conditions without resorting to a mixed formulation causes a reduction by one order in the convergence rates, while the mixed formulation maintains optimality of the error. See [5] for more details in the case of piecewise linear interpolation spaces. Similar results are expected for higher-order polynomials. We will soon report on the numerical analysis of the high-order SBM with Neumann boundary conditions in a separate publication.*

3. The High-Order Shifted Boundary Method for the Poisson Equation

In order to present the essential ingredients of high-order SBM, we start from the simplest case of the Poisson equation. We aim at numerically solving the Dirichlet boundary value problem

$$\begin{aligned} -\Delta u &= f \quad \text{in } \Omega\,, \\ u &= g \quad \text{on } \Gamma\,, \end{aligned} \tag{12}$$

where the data satisfy $f \in H^{m-1}(\Omega)$ and $g \in H^{m+1/2}(\Gamma)$ for some $m \geq 1$.

Introducing the finite dimensional subspace of $H^1(\tilde{\Omega}_h)$ made of continuous, piecewise polynomial functions on the triangulation $\tilde{\mathscr{T}}_h$,

$$V_h = V_h(\tilde{\Omega}_h; \tilde{\mathscr{T}}_h) := \{v \in H^1(\tilde{\Omega}_h) : v_{|T} \in \mathbb{P}_m(T),\ \forall T \in \tilde{\mathscr{T}}_h\}\,, \tag{13}$$

we discretize Problem (12) in $\tilde{\Omega}_h$ rather than Ω and enforce (9) on $\tilde{\Gamma}_h$ through Nitsche's penalization method [46]. Our weak form then reads:

Find $u_h \in V_h$ *such that* $\forall v_h \in V_h$

$$\begin{aligned} (\nabla u_h, \nabla v_h)_{0,\tilde{\Omega}_h} - (\partial_{\tilde{n}} u_h, v_h)_{0,\tilde{\Gamma}_h} - (S_h^m u_h, \partial_{\tilde{n}} v_h)_{0,\tilde{\Gamma}_h} + \gamma\,(h^{-1} S_h^m u_h, S_h^1 v_h)_{0,\tilde{\Gamma}_h} \\ = (f, v_h)_{0,\tilde{\Omega}_h} - (g, \partial_{\tilde{n}} v_h)_{0,\tilde{\Gamma}_h} + \gamma\,(h^{-1} g, S_h^1 v_h)_{0,\tilde{\Gamma}_h}\,, \end{aligned} \tag{14}$$

where the Nitsche parameter $\gamma > 0$ will be chosen large enough to guarantee the well-posedness of the problem.

Remark 3. *The SBM formulation for linear finite elements ($m = 1$) has been thoroughly investigated in [2]. For $m > 1$ note that the term $S_h^1 v_h$ appears in the Nitsche's penalty term. We could have replaced it with $S_h^m v_h$, but our specific choice is helpful in deriving an enhanced L^2 error estimate using the Aubin-Nitsche duality argument (see Sect. 9).*

In view of the subsequent analysis, it is convenient to introduce the bilinear form

$$a_h(u, v) := (\nabla u, \nabla v)_{0,\tilde{\Omega}_h} - (\partial_{\tilde{n}} u, v)_{0,\tilde{\Gamma}_h} - (S_h^m u, \partial_{\tilde{n}} v)_{0,\tilde{\Gamma}_h} + \gamma\,(h^{-1} S_h^m u, S_h^1 v)_{0,\tilde{\Gamma}_h} \tag{15}$$

and the linear form

$$\ell_h(v) := (f, v)_{0,\tilde{\Omega}_h} - (g, \partial_{\tilde{n}} v)_{0,\tilde{\Gamma}_h} + \gamma\,(h^{-1} g, S_h^1 v)_{0,\tilde{\Gamma}_h}\,, \tag{16}$$

so that the proposed SBM discretization can be written in compact form as follows:

$$\textit{Find } u_h \in V_h \textit{ such that} \qquad a_h(u_h, v_h) = \ell_h(v_h) \quad \forall v_h \in V_h\,. \tag{17}$$

Conditions on the well-posedness of this problem will be discussed in Sects. 5 and 6.

4. The High-Order Shifted Boundary Method for the Stokes Equations

The strong form of the Stokes flow equations with non-homogeneous Dirichlet and Neumann boundary conditions read

$$-\nabla \cdot (2\mu\, \boldsymbol{\varepsilon}(\boldsymbol{u}) - p\boldsymbol{I}) = \boldsymbol{f} \qquad \text{in } \Omega\,, \tag{18a}$$

$$\nabla \cdot \boldsymbol{u} = 0 \qquad \text{in } \Omega\,, \tag{18b}$$

$$\boldsymbol{u} = \boldsymbol{u}_D \qquad \text{on } \Gamma_D\,, \tag{18c}$$

$$(2\mu\,\boldsymbol{\varepsilon}(\boldsymbol{u}) - p\boldsymbol{I}) \cdot \boldsymbol{n} = \boldsymbol{t}_N \qquad \text{on } \Gamma_N\,, \tag{18d}$$

where $\boldsymbol{\varepsilon}(\boldsymbol{u}) = 1/2(\nabla\boldsymbol{u} + \nabla\boldsymbol{u}^T)$ is the velocity strain tensor (i.e., the symmetric gradient of the velocity), $\mu > 0$ is the dynamic viscosity, p is the pressure, $\boldsymbol{f} \in (H^{m-1}(\Omega))^n$ is a body force, $\boldsymbol{u}_D \in (H^{m+1/2}(\Gamma_D))^n$ is the value of the velocity on the Dirichlet boundary $\Gamma_D \neq \emptyset$ and $\boldsymbol{t}_N \in (H^{m-1/2}(\Gamma_N))^n$ is the vector-valued normal stress on the Neumann boundary Γ_N (where $\partial\Omega = \Gamma = \overline{\Gamma_D \cup \Gamma_N}$ with $\Gamma_D \cap \Gamma_N = \emptyset$). The Stokes flow represents a prototype for the application of the SBM to systems of differential equations in mixed form.

We introduce next the discrete spaces $\boldsymbol{V}_h(\tilde{\Omega}_h)$ and $Q_h(\tilde{\Omega}_h)$, for the velocity and the pressure, respectively. We assume that a stable and convergent base formulation for the Stokes flow exist for these spaces in the case of body-fitted grids. In what follows, for easiness of implementation we will consider the equal-order piecewise polynomial spaces

$$\boldsymbol{V}_h = \boldsymbol{V}_h(\tilde{\Omega}_h; \tilde{\mathscr{T}}_h) := \{\boldsymbol{v} \in H^1(\tilde{\Omega}_h)^n : \boldsymbol{v}_{|T} \in \mathbb{P}_m(T)^n,\ \forall T \in \tilde{\mathscr{T}}_h\}\,, \tag{19a}$$

$$Q_h = Q_h(\tilde{\Omega}_h; \tilde{\mathscr{T}}_h) := \{q \in H^1(\tilde{\Omega}_h) : q_{|T} \in \mathbb{P}_m(T),\ \forall T \in \tilde{\mathscr{T}}_h\}\,, \tag{19b}$$

for some $m \geq 1$, which will be coupled with the stabilized formulation of Hughes *et al.* [35]. Alternative choices are possible, such as, for example, using inf-sup stable Taylor-Hood elements with pressures of degree $m-1$ when $m \geq 2$, or using discontinuous Galerkin spaces.

In the case of pure Dirichlet conditions, that is $\Gamma_N = \emptyset$, the space $Q_h(\tilde{\Omega}_h)$ needs to be modified as

$$Q_h(\tilde{\Omega}_h) = \left\{ q_h \in Q_h(\tilde{\Omega}_h) \mid \int_{\tilde{\Omega}_h} q_h = 0 \right\}. \tag{20}$$

It is also convenient to introduce the product space $\boldsymbol{W}_h(\tilde{\Omega}_h) = \boldsymbol{V}_h(\tilde{\Omega}_h) \times Q_h(\tilde{\Omega}_h)$.

Discretizing Problem (18) in $\tilde{\Omega}_h$, enforcing (11) on $\tilde{\Gamma}_{D,h}$ with $\bar{\boldsymbol{g}} = \bar{\boldsymbol{u}}_D$, applying (18d) on Γ_N (see Assumption 1) and adopting an anti-symmetric form of the velocity strain and pressure gradient terms, we deduce the following SBM weak form of (18):

Find $[\boldsymbol{u}_h, p_h] \in \boldsymbol{W}_h$ *such that,* $\forall [\boldsymbol{w}_h, q_h] \in \boldsymbol{W}_h$

$$\begin{aligned}
&(2\mu\,\boldsymbol{\varepsilon}(\boldsymbol{u}_h), \boldsymbol{\varepsilon}(\boldsymbol{w}_h))_{0,\tilde{\Omega}_h} - (p_h, \nabla\cdot\boldsymbol{w}_h)_{0,\tilde{\Omega}_h} + (\nabla\cdot\boldsymbol{u}_h, q_h)_{0,\tilde{\Omega}_h} - (2\mu\,\boldsymbol{\varepsilon}(\boldsymbol{u}_h) - p_h\boldsymbol{I}, \boldsymbol{w}_h \otimes \tilde{\boldsymbol{n}})_{0,\tilde{\Gamma}_{D,h}} \\
&- (\boldsymbol{S}_h^m\boldsymbol{u}_h \otimes \tilde{\boldsymbol{n}}, 2\mu\,\boldsymbol{\varepsilon}(\boldsymbol{w}_h) + q_h\boldsymbol{I})_{0,\tilde{\Gamma}_{D,h}} + \gamma\,(2\mu\,h_\perp^{-1}\boldsymbol{S}_h^m\boldsymbol{u}_h, \boldsymbol{S}_h^1\boldsymbol{w}_h)_{0,\tilde{\Gamma}_{D,h}} \\
&+ \delta \sum_{T\in\tilde{\mathscr{T}}_h} \left(h_\tau^2\,(2\mu)^{-1}(-\nabla\cdot(2\mu\,\boldsymbol{\varepsilon}(\boldsymbol{u}_h)) + \nabla p_h), \nabla q_h\right)_{0,T} = (\boldsymbol{f}, \boldsymbol{w}_h)_{0,\tilde{\Omega}_h} + (\boldsymbol{t}_N, \boldsymbol{w}_h)_{0,\Gamma_{N,h}} \\
&- (\bar{\boldsymbol{u}}_D \otimes \tilde{\boldsymbol{n}}, 2\mu\,\boldsymbol{\varepsilon}(\boldsymbol{w}_h) + q_h\boldsymbol{I})_{0,\tilde{\Gamma}_{D,h}} + \gamma\,(2\mu\,h_\perp^{-1}\bar{\boldsymbol{u}}_D, \boldsymbol{S}_h^1\boldsymbol{w}_h)_{0,\tilde{\Gamma}_{D,h}} + \delta \sum_{T\in\tilde{\mathscr{T}}_h} \left(h_\tau^2\,(2\mu)^{-1}\boldsymbol{f}, \nabla q_h\right)_{0,T}\,,
\end{aligned} \tag{21}$$

where again $\gamma > 0$ is the Nitsche penalization parameter, whereas the parameter $\delta > 0$ scales a pressure stabilization term required by equal-order velocity/pressure pairs [35].

Remark 4. *As for the Poisson case, note that the term $S_h^1 \boldsymbol{v}_h$ appears in the Nitsche penalty term. We could have replaced it with $S_h^m \boldsymbol{v}_h$, but our specific choice is helpful in deriving a L^2 error estimate using the Aubin-Nitsche duality argument.*

In view of the subsequent analysis, it is convenient to introduce the bilinear form

$$\mathscr{B}_h([\boldsymbol{u}, p]; [\boldsymbol{w}, q]) := a_h(\boldsymbol{u}, \boldsymbol{w}) + b_h(p, \boldsymbol{w}) - b_h(q, \boldsymbol{u}) - \bar{b}_h(\boldsymbol{u}, q) + c_h(p, q)\,, \tag{22a}$$

with

$$a_h(\boldsymbol{u}, \boldsymbol{w}) := (2\mu\,\boldsymbol{\varepsilon}(\boldsymbol{u}), \boldsymbol{\varepsilon}(\boldsymbol{w}))_{0,\tilde{\Omega}_h} - (2\mu\,\boldsymbol{\varepsilon}(\boldsymbol{u}), \boldsymbol{w} \otimes \tilde{\boldsymbol{n}})_{0,\tilde{\Gamma}_{D,h}} - (\boldsymbol{S}_h^m\boldsymbol{u} \otimes \tilde{\boldsymbol{n}}, 2\mu\,\boldsymbol{\varepsilon}(\boldsymbol{w}))_{0,\tilde{\Gamma}_{D,h}} + \gamma\,(2\mu\,h^{-1}\,\boldsymbol{S}_h^m\boldsymbol{u}, \boldsymbol{S}_h^1\boldsymbol{w})_{0,\tilde{\Gamma}_{D,h}}\,, \tag{22b}$$

$$b_h(p, \boldsymbol{w}) := -(p, \nabla \cdot \boldsymbol{w})_{0,\tilde{\Omega}_h} + (p, \boldsymbol{w} \cdot \tilde{\boldsymbol{n}})_{0,\tilde{\Gamma}_{D,h}} , \tag{22c}$$

$$\bar{b}_h(\boldsymbol{u}, q) := \sum_{i=1}^{m} \left(\frac{\mathscr{D}_{\boldsymbol{d}}^i \boldsymbol{u}}{i!}, q\tilde{\boldsymbol{n}} \right)_{0,\tilde{\Gamma}_{D,h}} + \delta \sum_{T \in \tilde{\mathscr{T}}_h} \left(h^2 (2\mu)^{-1} \nabla \cdot (2\mu\, \boldsymbol{\varepsilon}(\boldsymbol{u})), \nabla q \right)_{0,T} , \tag{22d}$$

$$c_h(p_h, q_h) := \delta\, (h^2 (2\mu)^{-1} \nabla p, \nabla q)_{0,\tilde{\Omega}_h} , \tag{22e}$$

and the linear form

$$\mathscr{L}_h([\boldsymbol{w}, q]) := l_f(\boldsymbol{w}) + l_g(q) , \tag{22f}$$

with

$$l_f(\boldsymbol{w}) := (\boldsymbol{f}, \boldsymbol{w})_{0,\tilde{\Omega}_h} - (\bar{\boldsymbol{u}}_D \otimes \tilde{\boldsymbol{n}}, 2\mu\, \boldsymbol{\varepsilon}(\boldsymbol{w}))_{0,\tilde{\Gamma}_{D,h}} + \gamma\, (2\mu\, h^{-1}\, \bar{\boldsymbol{u}}_D, \boldsymbol{S}_h^1 \boldsymbol{w})_{0,\tilde{\Gamma}_{D,h}} + (\boldsymbol{t}_N, \boldsymbol{w})_{0,\Gamma_{N,h}} , \tag{22g}$$

$$l_g(q) := -(\bar{\boldsymbol{u}}_D \cdot \tilde{\boldsymbol{n}}, q)_{0,\tilde{\Gamma}_{D,h}} + \delta\, (h^2 (2\mu)^{-1} \boldsymbol{f}, \nabla q)_{0,\tilde{\Omega}_h} . \tag{22h}$$

So, the variational statement (21) can be succinctly expressed as:

Find $[\boldsymbol{u}_h, p_h] \in \boldsymbol{W}_h$ such that, $\forall [\boldsymbol{w}_h, q_h] \in \boldsymbol{W}_h$,

$$\mathscr{B}_h([\boldsymbol{u}_h, p_h]; [\boldsymbol{w}_h, q_h]) = \mathscr{L}_h([\boldsymbol{w}_h, q_h]) . \tag{23}$$

The study of well-posedness for this problem will be the object of the two following sections.

5. Coercivity and inf-sup properties of the bilinear forms

In this section, we give sufficient conditions that guarantee the uniform coercivity of the forms a_h for both the Poisson and the Stokes problem, and the fulfillment of a uniform inf-sup condition for the form $\mathscr{B}_h$ in the Stokes problem.

5.1. Poisson Problem

We start by making the following assumption on the distance between the surrogate and physical boundaries, in which the constant C_I is defined in Property 3 while the constant C_{inv} is defined in Property 4 in the Appendix.

Assumption 2. *The distance function $\boldsymbol{d}$ satisfies the condition*

$$\|h^{-1}\boldsymbol{d}\|_{L^\infty(\tilde{\Gamma}_h)} + \sum_{i=2}^{m} \frac{\|h^{-1}\boldsymbol{d}\|^i_{L^\infty(\tilde{\Gamma}_h)}}{i!} \leq \frac{\beta}{C_I} , \tag{24}$$

for some $\beta \in (0, 1)$.

Remark 5. *Assumption 2 was already used in [2] for the first-order polynomial interpolation space. In previous works [3–5], the authors used instead the assumption $\|\boldsymbol{d}\, h^{-1}\| \leq c_d h^\zeta$, for an arbitrary small $\zeta > 0$ and a fixed c_d, which implies Assumption 2, and for this reason is less general. Note, however, that this alternative approach does not depend on m. In fact, as $m \to \infty$, the left hand side of* (24) *converges to $e^{c_d h^\zeta} - 1$. Then, for $h \leq (\ln(1 + \beta/C_I)/c_d)^{1/\zeta}$,* (24) *is satisfied for any order m.*

Remark 6. *Assumption 2 provides a simple mathematical condition that guarantees both the solvability of the variational equations* (17) *and* (23)*, respectively, and the control of the remainder in the Taylor expansion of the boundary terms. Assumption 2 is a sufficient, but by no means necessary condition for the well-posedness of the SBM, and, in fact, it is not applied in the numerical tests, in which the grids are refined by simply splitting every element edge into two sub-edges. Below, we detail a procedure to generate grids that satisfy Assumption 2:*

1. Select $0 < \beta < 1$.

2. Compute β/C_I with C_I defined as in Property 3 in the Appendix.

3. Loop over the surrogate edges and compute $\|\boldsymbol{d}\, h^{-1}\|$ at the quadrature points.

4. If $\|\boldsymbol{d}\, h^{-1}\| > \beta/C_I$, slightly shift the location of the nodes closer to the true boundary.

Similar strategies can be followed in the case of the Stokes flow equations (see, later on, Assumption 3).

Theorem 1 (Coercivity, Poisson)**.** *There exist real numbers $0 < \hat{\beta}(C_{inv}) < 1$ and $\hat{\eta}(C_{inv}) > 0$ depending on the constant C_{inv}, such that if Assumption 2 holds for $\beta = \hat{\beta}(C_{inv})$ and the Nitsche penalization parameter satisfies $\gamma = 2\, C_I\, \eta$ with $\eta = \hat{\eta}(C_{inv})$, then the bilinear form a_h defined in (15) satisfies*

$$a_h(u_h, u_h) \geq \alpha\, \|u_h\|_a^2 \,, \qquad \forall u_h \in V_h \,, \tag{25a}$$

for some $\alpha = \hat{\alpha}(C_I\,,\, C_{inv}) > 0$, where

$$\|u\|_a^2 := \|\nabla u\|^2_{0,\tilde{\Omega}_h} + \|h^{-1/2} S_h^1 u\|^2_{0,\tilde{\Gamma}_h} \,. \tag{25b}$$

Proof. One has

$$\begin{aligned} a_h(v_h, v_h) &= \|\nabla v_h\|^2_{0,\tilde{\Omega}_h} - 2(S_h^1 v_h, \partial_{\tilde{n}} v_h)_{0,\tilde{\Gamma}_h} + (\partial_{\boldsymbol{d}} v_h, \partial_{\tilde{n}} v_h)_{0,\tilde{\Gamma}_h} \\ &\quad - \sum_{i=2}^{m} (\frac{\mathscr{D}^i_{\boldsymbol{d}} v_h}{i!}, \partial_{\tilde{\boldsymbol{n}}} v_h)_{0,\tilde{\Gamma}_h} + \gamma\, \|h^{-1/2} S_h^1 v_h\|^2_{0,\tilde{\Gamma}_h} + \gamma \sum_{i=2}^{m} (h^{-1} \frac{\mathscr{D}^i_{\boldsymbol{d}} v_h}{i!}, S_h^1 v_h)_{0,\tilde{\Gamma}_h} \\ &= \|\nabla v_h\|^2_{0,\tilde{\Omega}_h} - 2(h^{-1/2} S_h^1 v_h, h^{1/2} \partial_{\tilde{n}} v_h)_{0,\tilde{\Gamma}_h} + (h^{-1} \|\boldsymbol{d}\| h^{1/2}\, \partial_{\nu} v_h, h^{1/2}\, \partial_{\tilde{n}} v_h)_{0,\tilde{\Gamma}_h} \\ &\quad - \sum_{i=2}^{m} (h^{-1/2} \frac{\mathscr{D}^i_{\boldsymbol{d}} v_h}{i!}, h^{1/2} \partial_{\tilde{\boldsymbol{n}}} v_h)_{0,\tilde{\Gamma}_h} + \gamma\, \|h^{-1/2} S_h^1 v_h\|^2_{0,\tilde{\Gamma}_h} + \gamma \sum_{i=2}^{m} (h^{-1/2} \frac{\mathscr{D}^i_{\boldsymbol{d}} v_h}{i!}, h^{-1/2} S_h^1 v_h)_{0,\tilde{\Gamma}_h} \end{aligned} \tag{26}$$

From Property 3 and (116), we get

$$\begin{aligned} a_h(v_h, v_h) &\geq \|\nabla v_h\|^2_{0,\tilde{\Omega}_h} - 2 C_I^{1/2} \|h^{-1/2} S_h^1 v_h\|_{0,\tilde{\Gamma}_h} \|\nabla v_h\|_{0,\tilde{\Omega}_h} \\ &\quad - C_I\, \|\nabla v_h\|^2_{0,\tilde{\Omega}_h} \left(\|h^{-1} \boldsymbol{d}\|_{L^\infty(\tilde{\Gamma}_h)} + C_{inv}^{1/2} \sum_{i=2}^{m} \frac{\|h^{-1} \boldsymbol{d}\|^i_{L^\infty(\tilde{\Gamma}_h)}}{i!} \right) \\ &\quad + \gamma\, \|h^{-1/2} S_h^1 v_h\|^2_{0,\tilde{\Gamma}_h} - \gamma\, C_I^{1/2} C_{inv}^{1/2} \sum_{i=2}^{m} \frac{\|h^{-1} \boldsymbol{d}\|^i_{L^\infty(\tilde{\Gamma}_h)}}{i!} \|h^{-1/2} S_h^1 v_h\|_{0,\tilde{\Gamma}_h} \|\nabla v_h\|_{0,\tilde{\Omega}_h} \,, \end{aligned} \tag{27}$$

Note that here we abused slightly the notation, since C_{inv} refers to the largest of the inverse inequality constants associated with the derivatives in the term $\mathscr{D}^i_{\boldsymbol{d}} \boldsymbol{u}_h$ in (26). Similarly, we refer to C_I to the largest trace inequality constant, namely the one associated with ∇u_h. Whence, by Young's inequality,

$$\begin{aligned} a_h(v_h, v_h) &\geq \left[1 - C_I \left(\epsilon_1 + \|h^{-1} \boldsymbol{d}\|_{L^\infty(\tilde{\Gamma}_h)} + C_{inv}^{1/2} \sum_{i=2}^{m} \frac{\|h^{-1} \boldsymbol{d}\|^i_{L^\infty(\tilde{\Gamma}_h)}}{i!} \right) \right] \|\nabla v_h\|^2_{0,\tilde{\Omega}_h} \\ &\quad - 2^{-1} \gamma\, \epsilon_2\, C_I^{1/2} C_{inv}^{1/2} \sum_{i=2}^{m} \frac{\|h^{-1} \boldsymbol{d}\|^i_{L^\infty(\tilde{\Gamma}_h)}}{i!} \|\nabla v_h\|^2_{0,\tilde{\Omega}_h} \\ &\quad + \left(\gamma - \epsilon_1^{-1} - 2^{-1} \epsilon_2^{-1} \gamma\, C_I^{1/2} C_{inv}^{1/2} \sum_{i=2}^{m} \frac{\|h^{-1} \boldsymbol{d}\|^i_{L^\infty(\tilde{\Gamma}_h)}}{i!} \right) \|h^{-1/2} S_h^1 v_h\|^2_{0,\tilde{\Gamma}_h} \,. \end{aligned} \tag{28}$$

Choosing $\epsilon_1 = 2^{-1} C_I^{-1}$, $\epsilon_2 = C_I^{-1/2}$ and setting $\gamma = 2\, C_I\, \eta$ where $\eta > 0$ is a constant independent of the mesh size,

$$\begin{aligned} a_h(v_h, v_h)\eta \geq\, & 2^{-1} \|\nabla v_h\|^2_{0,\tilde{\Omega}_h} \\ & - C_I \left(\|h^{-1}\boldsymbol{d}\|_{L^\infty(\tilde{\Gamma}_h)} + (1+\eta)\, C_{inv}^{1/2} \sum_{i=2}^{m} \frac{\|h^{-1}\boldsymbol{d}\|^i_{L^\infty(\tilde{\Gamma}_h)}}{i!} \right) \|\nabla v_h\|^2_{0,\tilde{\Omega}_h} \\ & + 2\, C_I \left(\eta - 1 - 2^{-1} \eta\, C_I\, C_{inv}^{1/2} \sum_{i=2}^{m} \frac{\|h^{-1}\boldsymbol{d}\|^i_{L^\infty(\tilde{\Gamma}_h)}}{i!} \right) \|h^{-1/2} S_h^1 v_h\|^2_{0,\tilde{\Gamma}_h} . \end{aligned} \tag{29}$$

From Assumption 2, we obtain

$$a_h(v_h, v_h) \geq \left(2^{-1} - \beta \left(1 + (1+\eta)\, C_{inv}^{1/2}\right)\right) \|\nabla v_h\|^2_{0,\tilde{\Omega}_h} + 2\, C_I \left(\eta - 1 - 2^{-1} \eta\, C_{inv}^{1/2} \beta\right) \|h^{-1/2} S_h^1 v_h\|^2_{0,\tilde{\Gamma}_h} . \tag{30}$$

We need to find β so that 30 is positive, namely

$$\beta = \hat{\beta}(C_{inv}) < \min\left(2^{-1}(1 + (1+\eta)\, C_{inv}^{1/2})^{-1} \,,\, 2\,(\eta - 1)\, \eta^{-1} C_{inv}^{-1/2}\right) \,. \tag{31}$$

An optimal upper bound for β is attained by setting

$$\eta = \hat{\eta}(C_{inv}) = 8^{-1} C_{inv}^{-1/2} (-4 + C_{inv}^{1/2} + (65\, C_{inv} + 56\, C_{inv}^{1/2} + 16)^{1/2}) > 1 \,, \tag{32}$$

so that the quantities on the right hand side of (31) are equal. Thus, the result is attained with α being the smallest coefficient in (30), namely

$$\alpha = \hat{\alpha}(C_I \,,\, C_{inv}) = \min\left(2^{-1} - \beta \left(1 + (1+\eta)\, C_{inv}^{1/2}\right) \,,\, 2\, C_I \left(\eta - 1 - 2^{-1} \eta\, C_{inv}^{1/2} \beta\right)\right) \,. \tag{33}$$

□

Remark 7. *Since C_{inv} increases with m, then $\eta \to 8^{-1}(1 + 65^{1/2}) \approx 1.133$ as $m \to \infty$.*

Proposition 1. *The quantity $\|u_h\|_a$ defined in* (25b) *is a norm on $V_h(\tilde{\Omega}_h)$, equivalent to the norm $\|u_h\|_{1,\tilde{\Omega}_h}$ (although not uniformly with respect to the mesh size).*

Proof. The proof is the same as that of Theorem 7 in [4]. (See also Remark 9.) □

5.2. Stokes Problem

For the Stokes problem, we need a slightly stronger assumption on the distance between the surrogate and physical boundaries; hereafter, C_I and C_{inv} are defined as above, whereas $\bar{C}_K$ is the constant in Korn's inequality (117) in the Appendix.

Assumption 3. *The distance function $\boldsymbol{d}$ satisfies the condition*

$$\|h^{-1}\boldsymbol{d}\|_{L^\infty(\tilde{\Gamma}_h)} + \sum_{i=2}^{m} \frac{\|h^{-1}\boldsymbol{d}\|^i_{L^\infty(\tilde{\Gamma}_h)}}{i!} \leq \frac{\beta}{2^{1/2}\,\lambda} \,, \tag{34}$$

where, for some $\chi \in (0,1)$, $\lambda = (1-\chi^2)^{-1/2} C_I\, \bar{C}_K^{1/2}$ and $\beta = \chi \min\left(1, C_I^{1/2}(1-\chi^2)^{-1/2}\right)$.

To prove coercivity, we need an intermediate technical result.

Lemma 1. *Let Assumption 3 hold. Then, $\forall \boldsymbol{u}_h \in \boldsymbol{V}_h$,*

$$l(\tilde{\Omega}_h)^{-2} \|\boldsymbol{u}_h\|^2_{0,\tilde{\Omega}_h} + \left(1 - \chi^2\right) \|\nabla \boldsymbol{u}_h\|^2_{0,\tilde{\Omega}_h} \leq\; 2\, \bar{C}_K \|h^{-1/2} \boldsymbol{S}_h^1 \boldsymbol{u}_h\|^2_{0,\tilde{\Gamma}_{D,h}} + \bar{C}_K \|\boldsymbol{\varepsilon}(\boldsymbol{u}_h)\|^2_{0,\tilde{\Omega}_h} \,. \tag{35}$$

Proof. Korn's inequality (117) on the velocity $\boldsymbol{u}_h$ yields

$$l(\tilde{\Omega}_h)^{-2}\|\boldsymbol{u}_h\|^2_{0,\tilde{\Omega}_h} + \|\nabla \boldsymbol{u}_h\|^2_{0,\tilde{\Omega}_h} \leq \bar{C}_K \left(l(\tilde{\Omega}_h)^{-1}\|\boldsymbol{u}_h\|^2_{0,\tilde{\Gamma}_{D,h}} + \|\boldsymbol{\varepsilon}(\boldsymbol{u}_h)\|^2_{0,\tilde{\Omega}_h} \right) . \tag{36}$$

Using the triangle inequality, Assumption 3 and Property 3 give

$$\begin{aligned} l(\tilde{\Omega}_h)^{-1/2}\|\boldsymbol{u}_h\|_{0,\tilde{\Gamma}_{D,h}} &\leq l(\tilde{\Omega}_h)^{-1/2} h_\Gamma^{1/2} \|h^{-1/2}\boldsymbol{u}_h\|_{0,\tilde{\Gamma}_{D,h}} \\ &\leq \|h^{-1/2}\boldsymbol{S}_h^1\boldsymbol{u}_h\|_{0,\tilde{\Gamma}_{D,h}} + \|h^{-1/2}\nabla\boldsymbol{u}_h\, \boldsymbol{d}\|_{0,\tilde{\Gamma}_{D,h}} \\ &\leq \|h^{-1/2}\boldsymbol{S}_h^1\boldsymbol{u}_h\|_{0,\tilde{\Gamma}_{D,h}} + C_I^{1/2}\|h^{-1}\boldsymbol{d}\|_{L^\infty(\tilde{\Gamma}_h)}\|\nabla\boldsymbol{u}_h\|_{0,\tilde{\Omega}_h} \\ &\leq \|h^{-1/2}\boldsymbol{S}_h^1\boldsymbol{u}_h\|_{0,\tilde{\Gamma}_{D,h}} + 2^{-1/2}\beta\,\lambda^{-1}C_I^{1/2}\|\nabla\boldsymbol{u}_h\|_{0,\tilde{\Omega}_h} . \end{aligned} \tag{37}$$

Thus,

$$l(\tilde{\Omega}_h)^{-1}\|\boldsymbol{u}_h\|^2_{0,\tilde{\Gamma}_{D,h}} \leq 2\left(\|h^{-1/2}\boldsymbol{S}_h^1\boldsymbol{u}_h\|^2_{0,\tilde{\Gamma}_{D,h}} + 2^{-1}\beta^2\lambda^{-2}C_I\|\nabla\boldsymbol{u}_h\|^2_{0,\tilde{\Omega}_h} \right). \tag{38}$$

Substituting (38) into (36) yields

$$l(\tilde{\Omega}_h)^{-2}\|\boldsymbol{u}_h\|^2_{0,\tilde{\Omega}_h} + \left(1 - \beta^2\lambda^{-2}\bar{C}_K C_I\right)\|\nabla\boldsymbol{u}_h\|^2_{0,\tilde{\Omega}_h} \leq 2\,\bar{C}_K\|h^{-1/2}\boldsymbol{S}_h^1\boldsymbol{u}_h\|^2_{0,\tilde{\Gamma}_{D,h}} + \bar{C}_K\|\boldsymbol{\varepsilon}(\boldsymbol{u}_h)\|^2_{0,\tilde{\Omega}_h} . \tag{39}$$

Replacing β and λ with their definitions completes the proof. □

The remainder of this section will be devoted to establishing an inf-sup condition for the form $\mathscr{B}_h$ defined in (22a).

Theorem 2 (LBB inf-sup condition, Stokes)**.** *There exist real numbers $0 < \hat{\chi}(C_{inv}, C_I) < 1$ and $\hat{\eta}(C_{inv}, C_I) > 0$ depending on the constants C_{inv} and C_I, such that if Assumption 3 holds for some $\chi < \hat{\chi}(C_{inv}, C_I)$, the Nitsche penalization parameter satisfies $\gamma = 2\,C_I\,\eta$ with $\eta = \hat{\eta}(C_{inv}, C_I)$ and the pressure stabilization $\delta = 3^{-1}C_{inv}^{-1}$, then there exists a constant $\alpha_{LBB} > 0$, independent of the mesh size, such that for any pair $[\boldsymbol{u}_h, p_h] \in \boldsymbol{W}_h$ one can find a pair $[\boldsymbol{w}_h, q_h] \in \boldsymbol{W}_h$ satisfying*

$$\mathscr{B}_h([\boldsymbol{u}_h, p_h]; [\boldsymbol{w}_h, q_h]) \geq \alpha_{LBB} |||[\boldsymbol{u}_h, p_h]|||_{\mathscr{B}} |||[\boldsymbol{w}_h, q_h]|||_{\mathscr{B}} , \tag{40}$$

where

$$|||[\boldsymbol{u}_h, p_h]|||^2_{\mathscr{B}} := \|\boldsymbol{u}_h\|^2_a + \|(2\mu)^{-1/2}p_h\|^2_{0,\tilde{\Omega}_h} + \|(2\mu)^{-1/2}h\,\nabla p_h\|^2_{0,\tilde{\Omega}_h} . \tag{41}$$

and

$$\|\boldsymbol{u}\|^2_a := l(\tilde{\Omega}_h)^{-2}\|(2\,\mu)^{1/2}\boldsymbol{u}_h\|^2_{0,\tilde{\Omega}_h} + \|(2\,\mu)^{1/2}\nabla\boldsymbol{u}_h\|^2_{0,\tilde{\Omega}_h} + \|(2\,\mu)^{1/2}h^{-1/2}\boldsymbol{S}_h^1\boldsymbol{u}_h\|^2_{0,\tilde{\Gamma}_{D,h}} . \tag{42}$$

Proof. Choosing first $[\boldsymbol{w}_h, q_h] = [\boldsymbol{u}_h, p_h]$ in (22a), one has

$$\begin{aligned} \mathscr{B}_h([\boldsymbol{u}_h, p_h]; [\boldsymbol{u}_h, p_h]) = {}& \|(2\,\mu)^{1/2}\boldsymbol{\varepsilon}(\boldsymbol{u}_h)\|^2_{0,\tilde{\Omega}_h} - 2\,(2\mu\,\boldsymbol{\varepsilon}(\boldsymbol{u}_h)\tilde{\boldsymbol{n}}, \boldsymbol{S}_h^1\boldsymbol{u}_h)_{0,\tilde{\Gamma}_{D,h}} + (2\mu\,\boldsymbol{\varepsilon}(\boldsymbol{u}_h)\tilde{\boldsymbol{n}}, \partial_{\boldsymbol{d}}\boldsymbol{u}_h)_{0,\tilde{\Gamma}_{D,h}} \\ & - \sum_{i=2}^m (2\mu\,\boldsymbol{\varepsilon}(\boldsymbol{u}_h)\tilde{\boldsymbol{n}}, \frac{\mathscr{D}^i_{\boldsymbol{d}}\boldsymbol{u}_h}{i!})_{0,\tilde{\Gamma}_{D,h}} + \gamma\sum_{i=2}^m (2\mu\,h^{-1}\frac{\mathscr{D}^i_{\boldsymbol{d}}\boldsymbol{u}_h}{i!}, \boldsymbol{S}_h^1\boldsymbol{u}_h)_{0,\tilde{\Gamma}_{D,h}} \\ & + \gamma\,\|(2\,\mu)^{1/2}h^{-1/2}\boldsymbol{S}_h^1\boldsymbol{u}_h\|^2_{0,\tilde{\Gamma}_{D,h}} - \sum_{i=1}^m (\frac{\mathscr{D}^i_{\boldsymbol{d}}\boldsymbol{u}_h}{i!}, p_h\tilde{\boldsymbol{n}})_{0,\tilde{\Gamma}_{D,h}} \\ & + \delta\sum_{T\in\tilde{\mathscr{T}}_h}\left(h^2(2\,\mu)^{-1}\nabla\cdot(2\mu\,\boldsymbol{\varepsilon}(\boldsymbol{u}_h)), \nabla p_h\right)_{0,T} + \delta\,\|h\,(2\,\mu)^{-1/2}\nabla p_h\|^2_{0;\tilde{\Omega}_h} . \end{aligned} \tag{43}$$

Applying Property 3 and Corollary 1 of the Appendix, we obtain

$$\mathscr{B}_h([\boldsymbol{u}_h, p_h]; [\boldsymbol{u}_h, p_h]) \geq \|(2\,\mu)^{1/2}\boldsymbol{\varepsilon}(\boldsymbol{u}_h)\|^2_{0,\tilde{\Omega}_h} - 2\,C_I^{1/2}\|(2\,\mu)^{1/2}h^{-1/2}\boldsymbol{S}_h^1\boldsymbol{u}_h\|_{0,\tilde{\Gamma}_{D,h}}\|(2\mu\,h)^{1/2}\boldsymbol{\varepsilon}(\boldsymbol{u}_h)\|_{0,\tilde{\Omega}_h}$$

$$
\begin{aligned}
&- C_I \,\|(2\,\mu)^{1/2}\boldsymbol{\varepsilon}(\boldsymbol{u}_h)\|_{0,\tilde{\Omega}_h}\|(2\,\mu)^{1/2}\nabla\boldsymbol{u}_h\|_{0,\tilde{\Omega}_h}\left(\|h^{-1}\boldsymbol{d}\|_{L^\infty(\tilde{\Gamma}_h)} + C_{inv}^{1/2}\sum_{i=2}^{m}\frac{\|h^{-1}\boldsymbol{d}\|^i_{L^\infty(\tilde{\Gamma}_h)}}{i!}\right)\\
&- \gamma\, C_I^{1/2}C_{inv}^{1/2}\sum_{i=2}^{m}\frac{\|h^{-1}\boldsymbol{d}\|^i_{L^\infty(\tilde{\Gamma}_h)}}{i!}\|(2\,\mu)^{1/2}h^{-1/2}\boldsymbol{S}_h^1\boldsymbol{u}_h\|_{0,\tilde{\Gamma}_h}\|(2\,\mu)^{1/2}\nabla\boldsymbol{u}_h\|_{0,\tilde{\Omega}_h}\\
&+ \gamma\,\|(2\,\mu)^{1/2}h^{-1/2}\boldsymbol{S}_h^1\boldsymbol{u}_h\|^2_{0,\tilde{\Gamma}_{D,h}} + \delta\,\|h\,(2\,\mu)^{-1/2}\nabla p_h\|^2_{0;\tilde{\Omega}_h}\\
&+ \delta\,\|h\,(2\,\mu)^{-1/2}\nabla p_h\|_{0;\tilde{\Omega}_h}\|h\,(2\,\mu)^{1/2}\nabla\cdot\boldsymbol{\varepsilon}(\boldsymbol{u}_h)\|_{0;\tilde{\Omega}_h}\\
&- \left(\|h^{-1}\boldsymbol{d}\|_{L^\infty(\tilde{\Gamma}_h)} + C_{inv}^{1/2}\sum_{i=2}^{m}\frac{\|h^{-1}\boldsymbol{d}\|^i_{L^\infty(\tilde{\Gamma}_h)}}{i!}\right)\|(2\mu)^{-1/2}p_h\|_{0,\tilde{\Omega}_h}\|(2\,\mu)^{1/2}\nabla\boldsymbol{u}_h\|_{0,\tilde{\Omega}_h}\,.
\end{aligned}
\tag{44}
$$

Note that here we abused slightly the notation, since C_{inv} refers to the largest of the inverse inequality constants associated with the derivatives in the term $\mathscr{D}^i_{\boldsymbol{d}}\boldsymbol{u}_h$ in (26). Similarly, we refer to C_I to the largest trace inequality constant, namely the one associated with $\nabla\boldsymbol{u}_h$. Whence, by Young's inequality,

$$
\begin{aligned}
\mathscr{B}_h([\boldsymbol{u}_h,p_h];[\boldsymbol{u}_h,p_h]) \geq{}& \left(1 - C_I\,\epsilon_1 - 2^{-1}\epsilon_4^{-1}\delta\,C_{inv}\right)\|(2\,\mu)^{1/2}\boldsymbol{\varepsilon}(\boldsymbol{u}_h)\|^2_{0,\tilde{\Omega}_h}\\
&- 2^{-1}C_I\,\epsilon_2\left(\|h^{-1}\boldsymbol{d}\|_{L^\infty(\tilde{\Gamma}_h)} + C_{inv}^{1/2}\sum_{i=2}^{m}\frac{\|h^{-1}\boldsymbol{d}\|^i_{L^\infty(\tilde{\Gamma}_h)}}{i!}\right)\|(2\,\mu)^{1/2}\boldsymbol{\varepsilon}(\boldsymbol{u}_h)\|^2_{0,\tilde{\Omega}_h}\\
&- 2^{-1}C_I\,\epsilon_2^{-1}\left(\|h^{-1}\boldsymbol{d}\|_{L^\infty(\tilde{\Gamma}_h)} + C_{inv}^{1/2}\sum_{i=2}^{m}\frac{\|h^{-1}\boldsymbol{d}\|^i_{L^\infty(\tilde{\Gamma}_h)}}{i!}\right)\|(2\,\mu)^{1/2}\nabla\boldsymbol{u}_h\|^2_{0,\tilde{\Omega}_h}\\
&- 2^{-1}C_I\,C_{inv}^{1/2}\gamma\,\epsilon_3\sum_{i=2}^{m}\frac{\|h^{-1}\boldsymbol{d}\|^i_{L^\infty(\tilde{\Gamma}_h)}}{i!}\|(2\,\mu)^{1/2}\nabla\boldsymbol{u}_h\|^2_{0,\tilde{\Omega}_h}\\
&+ \left(\gamma - \epsilon_1^{-1} - 2^{-1}\gamma\,\epsilon_3^{-1}C_{inv}^{1/2}\sum_{i=2}^{m}\frac{\|h^{-1}\boldsymbol{d}\|^i_{L^\infty(\tilde{\Gamma}_h)}}{i!}\right)\|(2\,\mu)^{1/2}h^{-1/2}\boldsymbol{S}_h^1\boldsymbol{u}_h\|^2_{0,\tilde{\Gamma}_{D,h}}\\
&+ \delta\left(1 - 2^{-1}\epsilon_4\right)\|h\,(2\,\mu)^{-1/2}\nabla p_h\|^2_{0;\tilde{\Omega}_h}\\
&- 2^{-1}\epsilon_5\,C_I\left(\|h^{-1}\boldsymbol{d}\|_{L^\infty(\tilde{\Gamma}_h)} + C_{inv}^{1/2}\sum_{i=2}^{m}\frac{\|h^{-1}\boldsymbol{d}\|^i_{L^\infty(\tilde{\Gamma}_h)}}{i!}\right)\|(2\mu)^{-1/2}p_h\|^2_{0,\tilde{\Omega}_h}\\
&- 2^{-1}\epsilon_5^{-1}C_I\left(\|h^{-1}\boldsymbol{d}\|_{L^\infty(\tilde{\Gamma}_h)} + C_{inv}^{1/2}\sum_{i=2}^{m}\frac{\|h^{-1}\boldsymbol{d}\|^i_{L^\infty(\tilde{\Gamma}_h)}}{i!}\right)\|(2\,\mu)^{1/2}\nabla\boldsymbol{u}_h\|^2_{0,\tilde{\Omega}_h}\,.
\end{aligned}
\tag{45}
$$

Choosing $\epsilon_1 = 2^{-1}C_I^{-1}$, $\epsilon_2 = \lambda\,C_I^{-1}$, $\epsilon_3 = 2^{-1}\lambda^{-1}$, $\epsilon_4 = 2\cdot 3^{-1}$, $\epsilon_5 = \epsilon_2$, $\delta = 3^{-1}C_{inv}^{-1}$ and $\gamma = 2\,C_I\,\eta$, yields

$$
\begin{aligned}
\mathscr{B}_h([\boldsymbol{u}_h,p_h];[\boldsymbol{u}_h,p_h]) \geq{}& 2^{-2}\|(2\,\mu)^{1/2}\boldsymbol{\varepsilon}(\boldsymbol{u}_h)\|^2_{0,\tilde{\Omega}_h}\\
&- 2^{-1}\lambda\left(\|h^{-1}\boldsymbol{d}\|_{L^\infty(\tilde{\Gamma}_h)} + C_{inv}^{1/2}\sum_{i=2}^{m}\frac{\|h^{-1}\boldsymbol{d}\|^i_{L^\infty(\tilde{\Gamma}_h)}}{i!}\right)\|(2\,\mu)^{1/2}\boldsymbol{\varepsilon}(\boldsymbol{u}_h)\|^2_{0,\tilde{\Omega}_h}\\
&- C_I^2\lambda^{-1}\left(\|h^{-1}\boldsymbol{d}\|_{L^\infty(\tilde{\Gamma}_h)} + \left(1 + 2^{-1}\eta\right)C_{inv}^{1/2}\sum_{i=2}^{m}\frac{\|h^{-1}\boldsymbol{d}\|^i_{L^\infty(\tilde{\Gamma}_h)}}{i!}\right)\|(2\,\mu)^{1/2}\nabla\boldsymbol{u}_h\|^2_{0,\tilde{\Omega}_h}\\
&+ 2\,C_I\left(\eta - 1 - \lambda\,\eta\,C_{inv}^{1/2}\sum_{i=2}^{m}\frac{\|h^{-1}\boldsymbol{d}\|^i_{L^\infty(\tilde{\Gamma}_h)}}{i!}\right)\|(2\,\mu)^{1/2}h^{-1/2}\boldsymbol{S}_h^1\boldsymbol{u}_h\|^2_{0,\tilde{\Gamma}_{D,h}}\\
&+ 2\cdot 3^{-1}\delta\,\|h\,(2\,\mu)^{-1/2}\nabla p_h\|^2_{0;\tilde{\Omega}_h}
\end{aligned}
$$

$$- 2^{-1} C_I \left(\|h^{-1}\boldsymbol{d}\|_{L^\infty(\tilde{\Gamma}_h)} + C_{inv}^{1/2} \sum_{i=2}^{m} \frac{\|h^{-1}\boldsymbol{d}\|^i_{L^\infty(\tilde{\Gamma}_h)}}{i!} \right) \|(2\mu)^{-1/2} p_h\|^2_{0,\tilde{\Omega}_h} . \tag{46}$$

From Assumption 3,

$$\begin{aligned}
\mathscr{B}_h([\boldsymbol{u}_h, p_h]; [\boldsymbol{u}_h, p_h]) \geq\; & 2^{-3/2} \left(2^{-1/2} - \beta\,(1 + C_{inv}^{1/2})\right) \|(2\,\mu)^{1/2} \boldsymbol{\varepsilon}(\boldsymbol{u}_h)\|^2_{0,\tilde{\Omega}_h} \\
& - 2^{-1/2} \lambda^{-2} C_I^2 \beta \left(1 + \left(1 + 2^{-1}\eta\right) C_{inv}^{1/2}\right) \|(2\,\mu)^{1/2} \nabla \boldsymbol{u}_h\|^2_{0,\tilde{\Omega}_h} \\
& + 2\, C_I \left(\eta - 1 - 2^{-1/2}\beta\,\eta\, C_{inv}^{1/2}\right) \|(2\,\mu)^{1/2} h^{-1/2} \boldsymbol{S}_h^1 \boldsymbol{u}_h\|^2_{0,\tilde{\Gamma}_{D,h}} \\
& + 2 \cdot 3^{-1} \delta\, \|h\,(2\,\mu)^{-1/2} \nabla p_h\|^2_{0;\tilde{\Omega}_h} - 2^{-3/2} \lambda^{-1} C_I\,(1 + C_{inv}^{1/2})\,\beta\, \|(2\mu)^{-1/2} p_h\|^2_{0,\tilde{\Omega}_h} .
\end{aligned} \tag{47}$$

Making sure $\beta < 2^{-1/2}(1 + C_{inv}^{1/2})^{-1}$, applying Lemma 1 to the first term on the right-hand side, and recalling the definition of λ, we obtain

$$\begin{aligned}
\mathscr{B}_h([\boldsymbol{u}_h, p_h]; [\boldsymbol{u}_h, p_h]) \geq\; & 2^{-3/2} \bar{C}_K^{-1} \left(1 - \chi^2\right) \left(2^{-1/2} - \beta(3\,(1 + C_{inv}^{1/2}) + \eta\, C_{inv}^{1/2})\right) \|(2\,\mu)^{1/2} \nabla \boldsymbol{u}_h\|^2_{0,\tilde{\Omega}_h} \\
& + 2^{-3/2} \bar{C}_K^{-1} \left(1 - \chi^2\right) \left(2^{-1/2} - \beta\,(1 + C_{inv}^{1/2})\right) l(\tilde{\Omega}_h)^{-2} \|(2\,\mu)^{1/2} \boldsymbol{u}_h\|^2_{0,\tilde{\Omega}_h} \\
& + 2\, C_I \left(\eta - 1 - 2^{-1/2}\beta\,\eta\, C_{inv}^{1/2} - 2^{-3/2} C_I^{-1} (2^{-1/2} - \beta\,(1 + C_{inv}^{1/2}))\right) \|(2\,\mu)^{1/2} h^{-1/2} \boldsymbol{S}_h^1 \boldsymbol{u}_h\|^2_{0,\tilde{\Gamma}_{D,h}} \\
& + 2 \cdot 3^{-1} \delta\, \|h\,(2\,\mu)^{-1/2} \nabla p_h\|^2_{0;\tilde{\Omega}_h} - 2^{-3/2} \bar{C}_K^{-1/2} (1 - \chi^2)^{1/2} (1 + C_{inv}^{1/2})\, \|(2\mu)^{-1/2} p_h\|^2_{0,\tilde{\Omega}_h} .
\end{aligned} \tag{48}$$

We need to find β so that 48 is positive, namely

$$\beta < \min \left(2^{-1/2} \left(3\,(1 + C_{inv}^{1/2}) + \eta\, C_{inv}^{1/2}\right)^{-1} ,\; 2^{1/2} \left(\eta - 1 - 2^{-2} C_I^{-1}\right) \left(\eta\, C_{inv}^{1/2} - 2^{-1} C_I^{-1} (1 + C_{inv}^{1/2})\right)^{-1} \right) . \tag{49}$$

From the definition of β one can satisfy (49) by picking

$$\chi < \min \left(2^{-1/2} \left(3\,(1 + C_{inv}^{1/2}) + \eta\, C_{inv}^{1/2}\right)^{-1} ,\; 2^{1/2} \left(\eta - 1 - 2^{-2} C_I^{-1}\right) \left(\eta\, C_{inv}^{1/2} - 2^{-1} C_I^{-1} (1 + C_{inv}^{1/2})\right)^{-1} \right) . \tag{50}$$

An optimal upper bound for χ is attained by setting

$$\eta = -2^{-1} \left(3\, C_{inv}^{-1/2} + 3 \cdot 2^{-1} - 4^{-1} C_I^{-1}\right) + \left(4^{-1} (3\, C_{inv}^{-1/2} + 3 \cdot 2^{-1} - 4^{-1} C_I^{-1})^2 + (1 + C_{inv}^{-1/2})(3 + 2^{-1} C_I^{-1})\right)^{1/2} , \tag{51}$$

so that the quantities on the right hand side of (50) are equal. Thus, with α being the smallest positive coefficient in (48),

$$\mathscr{B}_h([\boldsymbol{u}_h, p_h]; [\boldsymbol{u}_h, p_h]) \geq \alpha\, \|\boldsymbol{u}_h\|^2_a + \alpha\, \|h\,(2\,\mu)^{-1/2} \nabla p_h\|^2_{0;\tilde{\Omega}_h} - 2^{-3/2} \bar{C}_K^{-1/2} (1 - \chi^2)^{1/2} (1 + C_{inv}^{1/2})\,\beta\, \|(2\mu)^{-1/2} p_h\|^2_{0,\tilde{\Omega}_h} \tag{52}$$

with $\|\boldsymbol{u}_h\|_a$ as defined in (42). At this point, we follow the same steps detailed in Theorem 3 in [3]. In particular, there exists a constant $C_{LBB} > 0$ independent of the meshsize, and an element $\boldsymbol{v}^{p_h} \in (H^1_{0,\tilde{\Gamma}_{D,h}}(\tilde{\Omega}_h))^n$ satisfying $-(p_h, \nabla \cdot \boldsymbol{v}^{p_h})_{\tilde{\Omega}_h} \geq C_{LBB}\, \|p_h\|_{0;\tilde{\Omega}_h} \|\boldsymbol{v}^{p_h}\|_{1,\tilde{\Omega}_h}$ with $l(\tilde{\Omega}_h)^{-1} \|(2\mu)^{1/2}\, \boldsymbol{v}^{p_h}\|_{1;\tilde{\Omega}_h} = \|(2\mu)^{-1/2} p_h\|_{0;\tilde{\Omega}_h}$. Let $\boldsymbol{v}_h^{p_h}$ be the H^1-continuous finite element interpolant of $\boldsymbol{v}^{p_h}$ defined by the Scott-Zhang operator; then $l(\tilde{\Omega}_h)^{-1} \|(2\mu)^{1/2}\, \boldsymbol{v}^{p_h}\|_{1;\tilde{\Omega}_h} \leq C_{SZC}\, \|(2\mu)^{-1/2} p_h\|_{0;\tilde{\Omega}_h}$. Taking $[\boldsymbol{w}, q] = [\boldsymbol{v}_h^{p_h}, 0]$ in (22a) and using the fact that the trace of $\boldsymbol{v}^{p_h}$ and $\boldsymbol{v}_h^{p_h}$ on $\tilde{\Gamma}_{D,h}$ is zero, we have

$$\begin{aligned}
\mathscr{B}_h([\boldsymbol{u}_h, p_h]; [\boldsymbol{v}_h^{p_h}, 0]) &= a(\boldsymbol{u}_h, \boldsymbol{v}_h^{p_h}) + b(p_h, \boldsymbol{v}_h^{p_h}) \\
&= (2\mu\, \boldsymbol{\varepsilon}(\boldsymbol{u}_h), \boldsymbol{\varepsilon}(\boldsymbol{v}_h^{p_h}))_{0,\tilde{\Omega}_h} - (\nabla \cdot (\boldsymbol{v}_h^{p_h} - \boldsymbol{v}^{p_h}), p_h)_{0,\tilde{\Omega}_h} - (\nabla \cdot \boldsymbol{v}^{p_h}, p_h)_{0,\tilde{\Omega}_h} \\
&\quad - (\boldsymbol{S}_h^m \boldsymbol{u}_h \otimes \tilde{\boldsymbol{n}}, 2\mu\, \boldsymbol{\varepsilon}(\boldsymbol{v}_h^{p_h}))_{0,\tilde{\Gamma}_{D,h}} + \gamma\,(2\mu\, h^{-1} \boldsymbol{S}_h^m \boldsymbol{u}_h, \nabla \boldsymbol{v}_h^{p_h}\, \boldsymbol{d})_{0,\tilde{\Gamma}_{D,h}} .
\end{aligned} \tag{53}$$

The first three terms can be bounded similarly to Theorem 3 in [3]:

$$(\boldsymbol{\varepsilon}(\boldsymbol{v}_h^{p_h}), 2\mu\, \boldsymbol{\varepsilon}(\boldsymbol{u}_h))_{0,\tilde{\Omega}_h} \geq -2^{-1}\epsilon_6^{-1} \| \sqrt{2\mu}\, \nabla \boldsymbol{u}_h\|^2_{0;\tilde{\Omega}_h} - 2^{-1} C_{SZC}\, \epsilon_6 \|p_h/\sqrt{2\mu}\|^2_{0;\tilde{\Omega}_h} , \tag{54a}$$

$$-(\nabla\cdot(\boldsymbol{v}_h^{p_h} - \boldsymbol{v}^{p_h}), p_h)_{0,\tilde{\Omega}_h} \geq -2^{-1}\epsilon_7^{-1} \|(2\mu)^{-1/2} h\, \nabla p_h\|^2_{0;\tilde{\Omega}_h} - 2^{-1}\epsilon_7\, C_{SZC}\, C_{int}^2 \|(2\mu)^{-1/2} p_h\|^2_{0;\tilde{\Omega}_h} , \tag{54b}$$

$$-(\nabla\cdot \boldsymbol{v}^{p_h}, p_h)_{0,\tilde{\Omega}_h} \geq C_{LBB} \|(2\mu)^{-1/2} p_h\|^2_{0,\tilde{\Omega}_h} . \tag{54c}$$

Using Assumption 3, Corollary 1 and Property 3 in the Appendix, we can bound the last two terms in (53):

$$\begin{aligned}
-(\boldsymbol{S}_h^m \boldsymbol{u}_h \otimes \tilde{\boldsymbol{n}}, 2\mu\, \boldsymbol{\varepsilon}(\boldsymbol{v}_h^{p_h}))_{0,\tilde{\Gamma}_{D,h}} \geq\; & -2^{-1}\epsilon_8^{-1} \|(2\mu)^{1/2} h^{-1/2} \boldsymbol{S}_h^1 \boldsymbol{u}_h\|^2_{0;\tilde{\Gamma}_{D,h}} - 2^{-1}\epsilon_9^{-1} C_I\, C_{inv}^{1/2} \sum_{i=2}^{m} \frac{\|h^{-1}\boldsymbol{d}\|^i_{L^\infty(\tilde{\Gamma}_h)}}{i!} \|(2\mu)^{1/2}\nabla \boldsymbol{u}_h\|^2_{0;\tilde{\Omega}_h} \\
& -2^{-1} C_I\, \epsilon_8 \|(2\mu)^{1/2} \boldsymbol{\epsilon}(\boldsymbol{v}_h^{p_h})\|^2_{0;\tilde{\Omega}_h} - 2^{-1}\epsilon_9\, C_I\, C_{inv}^{1/2} \sum_{i=2}^{m} \frac{\|h^{-1}\boldsymbol{d}\|^i_{L^\infty(\tilde{\Gamma}_h)}}{i!} \|(2\mu)^{1/2} \boldsymbol{\epsilon}(\boldsymbol{v}_h^{p_h})\|^2_{0;\tilde{\Omega}_h} \\
\geq\; & -2^{-1}\epsilon_8^{-1} \|(2\mu)^{1/2} h^{-1/2} \boldsymbol{S}_h^1 \boldsymbol{u}_h\|^2_{0;\tilde{\Gamma}_{D,h}} - 2^{-3/2}\epsilon_9^{-1} \lambda^{-1} C_I\, \beta\, C_{inv}^{1/2} \|(2\mu)^{1/2}\nabla \boldsymbol{u}_h\|^2_{0;\tilde{\Omega}_h} \\
& -2^{-1} C_{SZC}\, C_I \left(\epsilon_8 + 2^{-1/2}\epsilon_9\, \lambda^{-1} C_{inv}^{1/2}\beta\right) \|(2\mu)^{-1/2} p_h\|^2_{0;\tilde{\Omega}_h} ,
\end{aligned} \tag{54d}$$

$$\begin{aligned}
\gamma\,(2\mu\, h^{-1} \boldsymbol{S}_h^m \boldsymbol{u}_h, \nabla \boldsymbol{v}_h^{p_h}\, \boldsymbol{d})_{0,\tilde{\Gamma}_{D,h}} \geq\; & -2^{-3/2}\gamma\, \lambda^{-1}\epsilon_{10}^{-1}\, \beta \|(2\mu)^{1/2} h^{-1/2} \boldsymbol{S}_h^1 \boldsymbol{u}_h\|^2_{0;\tilde{\Gamma}_{D,h}} - 2^{-2}\gamma\, \lambda^{-2}\epsilon_{11}^{-1} C_I\, C_{inv}^{1/2}\, \beta^2 \|(2\mu)^{1/2}\nabla \boldsymbol{u}_h\|^2_{0;\tilde{\Omega}_h} \\
& -\gamma\, 2^{-1} C_I \lambda^{-1}\beta \left(2^{-1/2}\epsilon_{10} + 2^{-1}\lambda^{-1}\beta\, C_{inv}^{1/2}\, \epsilon_{11}\right) \|(2\mu)^{1/2}\nabla \boldsymbol{v}_h^{p_h}\|^2_{0;\tilde{\Omega}_h} \\
\geq\; & -2^{-3/2}\gamma\, \lambda^{-1}\epsilon_{10}^{-1}\, \beta \|(2\mu)^{1/2} h^{-1/2} \boldsymbol{S}_h^1 \boldsymbol{u}_h\|^2_{0;\tilde{\Gamma}_{D,h}} - 2^{-2}\gamma\, \lambda^{-2}\epsilon_{11}^{-1} C_I\, C_{inv}^{1/2}\, \beta^2 \|(2\mu)^{1/2}\nabla \boldsymbol{u}_h\|^2_{0;\tilde{\Omega}_h} \\
& -\gamma\, 2^{-1} C_{SZC}\, C_I\, \lambda^{-1}\, \beta \left(2^{-1/2}\epsilon_{10} + 2^{-1}\, \lambda^{-1}\beta\, C_{inv}^{1/2}\epsilon_{11}\right) \|(2\mu)^{-1/2} p_h\|^2_{0;\tilde{\Omega}_h} .
\end{aligned} \tag{54e}$$

We can combine all the results obtained so far by choosing the test functions as $[\boldsymbol{w}_h, q_h] = [\zeta \boldsymbol{u}_h + \boldsymbol{v}_h^{p_h}, \zeta p_h]$ and taking $\epsilon_6 = 6^{-1} C_{SZC}^{-1} C_{LBB}$, $\epsilon_7 = C_{int}^{-2}\epsilon_6$, $\epsilon_8 = C_I^{-1}\epsilon_6$, $\epsilon_9 = 2^{1/2}\beta^{-1} C_{inv}^{-1/2}\lambda\, \epsilon_8$, $\epsilon_{10} = \gamma^{-1} C_{inv}^{1/2}\epsilon_9$ and $\epsilon_{11} = 2^{1/2}\beta^{-1}\lambda\, C_{inv}^{-1/2}\epsilon_{10}$; gives

$$\begin{aligned}
\mathscr{B}_h([\boldsymbol{u}_h, p_h]; [\zeta \boldsymbol{u}_h + \boldsymbol{v}_h^{p_h}, \zeta p_h]) \geq\; & \zeta\, \alpha \|(2\mu)^{1/2}\nabla \boldsymbol{u}_h\|^2_{0;\tilde{\Omega}_h} \\
& -3\, C_{LBB}^{-1} C_{SZC} \left(1 + 2^{-1} C_{inv}\, C_I^2 \beta^2 \lambda^{-2} + 2^{-2} C_{inv}\, \gamma^2 \lambda^{-4} C_I^2 \beta^4\right) \|(2\mu)^{1/2}\nabla \boldsymbol{u}_h\|^2_{0;\tilde{\Omega}_h} \\
& + \left(\zeta\, \alpha - 3\, C_{LBB}^{-1} C_{SZC}\, C_{int}^2\right) \|(2\mu)^{-1/2} h\, \nabla p_h\|^2_{0;\tilde{\Omega}_h} + \zeta\, \alpha \|(2\mu)^{1/2} h^{-1/2}\, \boldsymbol{S}_h^1 \boldsymbol{u}_h\|^2_{0;\tilde{\Gamma}_{D,h}} \\
& -3\, C_{LBB}^{-1} C_{SZC}\, C_I \left(1 + 2^{-1}\lambda^{-2}\gamma^2\beta^2\right) \|(2\mu)^{1/2} h^{-1/2}\, \boldsymbol{S}_h^1 \boldsymbol{u}_h\|^2_{0;\tilde{\Gamma}_{D,h}} \\
& + \left(2^{-1} C_{LBB} - \zeta\, 2^{-3/2} \bar{C}_K^{-1/2} (1-\chi^2)^{1/2} (1 + C_{inv}^{1/2})\beta\right) \|(2\mu)^{-1/2} p_h\|^2_{0;\tilde{\Omega}_h} \\
& + \zeta\, \alpha\, l(\tilde{\Omega}_h)^{-2} \|(2\mu)^{1/2} \boldsymbol{u}_h\|^2_{0,\tilde{\Omega}_h} .
\end{aligned} \tag{55}$$

Picking $\zeta > 3\, \alpha^{-1} C_{LBB}^{-1} C_{SZC}\, \rho$ with

$$\rho = \max\left(1 + 2^{-1} C_{inv}\, C_I^2 \beta^2 \lambda^{-2} + 2^{-2} C_{inv}\, \gamma^2 \lambda^{-4} C_I^2 \beta^4,\, C_{int}^2,\, C_I \left(1 + 2^{-1}\lambda^{-2}\gamma^2\beta^2\right)\right) \tag{56}$$

and selecting χ small enough such that $(1-\chi^2)^{1/2}\beta < 2^{1/2} C_{LBB}\, \zeta^{-1} \bar{C}_K^{1/2} (1 + C_{inv}^{1/2})^{-1}$, we can conclude the proof by taking the LBB constant equal to

$$\alpha_{LBB} := \min\left(\zeta C_b - 3\rho\, C_{LBB}^{-1} C_{SZC}\, ,\, 2^{-1} C_{LBB} - \zeta\, 2^{-3/2} \bar{C}_K^{-1/2} (1-\chi^2)^{1/2} (1 + C_{inv}^{1/2})\beta\right) . \tag{57}$$

□

Remark 8. *Since C_{inv} and C_I increase with m, then $\eta \to 4^{-1}(-3 + 57^{1/2}) \approx 1.138$ as $m \to \infty$.*

6. Continuity of the bilinear forms

In this section, we prove the continuity of the bilinear forms introduced in Sects. 3 and 4, with respect to the norms of suitable infinite-dimensional spaces of functions defined in $\tilde{\Omega}_h$.

6.1. Poisson Problem

In view of the convergence analysis, we consider a_h as defined on a product space $V(\tilde{\Omega}_h; \tilde{\mathcal{T}}_h) \times V(\tilde{\Omega}_h; \tilde{\mathcal{T}}_h)$, where $V(\tilde{\Omega}_h; \tilde{\mathcal{T}}_h)$ is an infinite-dimensional subspace of $H^1(\tilde{\Omega}_h)$, depending upon the triangulation $\tilde{\mathcal{T}}_h$ and containing V_h, made of functions for which the traces on $\tilde{\Gamma}_h$ of any partial derivative of order $\leq m$ is well-defined and controlled in $L^2(\tilde{\Gamma}_h)$.

To define $V(\tilde{\Omega}_h; \tilde{\mathcal{T}}_h)$, let us introduce a 'reference' element $\hat{T}$ for all our triangulations; as usual, we assume that $\hat{T}$ has unitary diameter. Let $\hat{E} \subset \partial\hat{T}$ any edge/face of $\hat{T}$. Given a function $v \in H^m(\hat{T})$, denote hereafter by $\hat{\partial}^i v$ any partial derivative of v of order $i \leq m$. Then, the trace theorem (see e.g. [29]) guarantees that for $0 \leq i \leq m-1$ the restriction $(\hat{\partial}^i v)_{|\hat{E}}$ belongs to $L^2(\hat{E})$; more precisely, there exists a constant $\hat{C} > 0$ such that $\|\hat{\partial}^i v\|^2_{0,\hat{E}} \leq \hat{C}\, \|v\|^2_{m,\hat{T}}$ for all $v \in H^m(\hat{T})$, $0 \leq i \leq m-1$. On the other hand, the norm on the right-hand side is equivalent to the norm $(\|v\|^2_{0,\hat{T}} + |v|^2_{m,\hat{T}})^{1/2}$; hence, after possibly changing the value of $\hat{C}$ it holds

$$\|\hat{\partial}^i v\|^2_{0,\hat{E}} \leq \hat{C}\left(\|v\|^2_{0,\hat{T}} + |v|^2_{m,\hat{T}}\right), \qquad \forall v \in H^m(\hat{T}), \qquad 0 \leq i \leq m-1\,.$$

Replacing v by any component of the gradient $\hat{\nabla} w$ of a function $w \in H^{m+1}(\hat{T})$ yields

$$\|\hat{\partial}^i w\|^2_{0,\hat{E}} \leq \hat{C}\left(\|\hat{\nabla} w\|^2_{0,\hat{T}} + |w|^2_{m+1,\hat{T}}\right), \qquad \forall w \in H^{m+1}(\hat{T}), \qquad 1 \leq i \leq m\,.$$

Next, consider an element $T \in \tilde{\mathcal{T}}_h$ with edge/face E: a mapping and scaling argument yields after a simple computation the existence of a constant $\bar{C}_I > 0$ independent of h such that

$$h_T^{2i-1}\|\partial^i w\|^2_{0,E} \leq \bar{C}_I\left(\|\nabla w\|^2_{0,T} + h_T^{2m}|w|^2_{m+1,T}\right), \qquad \forall w \in H^{m+1}(T), \qquad 1 \leq i \leq m\,, \tag{58}$$

where $\partial^i w$ denotes here any partial derivative of w of order i.

Based on this estimate, we are led to give the following definition of the space $V(\tilde{\Omega}_h; \tilde{\mathcal{T}}_h)$, which involves the strip of elements in $\tilde{\mathcal{T}}_h$ with at least one edge/face on $\tilde{\Gamma}_h$, i.e., the subset

$$\tilde{\Omega}^b_h := \bigcup\{T \in \tilde{\mathcal{T}}^b_h\}\,, \tag{59}$$

where $\tilde{\mathcal{T}}^b_h := \{T \in \tilde{\mathcal{T}}_h : \text{meas}\,(\partial T \cap \tilde{\Gamma}_h) > 0\}$.

Definition 1. *Let us set*

$$V(\tilde{\Omega}_h; \tilde{\mathcal{T}}_h) = V(\tilde{\Omega}_h; \tilde{\mathcal{T}}_h, m) := \{w \in H^1(\tilde{\Omega}_h) : w_{|T} \in H^{m+1}(T), \;\; \forall T \in \tilde{\mathcal{T}}^b_h\}\,, \tag{60}$$

equipped with the norm

$$\|w\|^2_{V(\tilde{\Omega}_h;\tilde{\mathcal{T}}_h)} := \|w\|^2_a \,+\, |h^m\, w|^2_{m+1,\tilde{\mathcal{T}}^b_h}\,. \tag{61}$$

Note that $V_h \subset V(\tilde{\Omega}_h; \tilde{\mathcal{T}}_h)$ and $\|v_h\|_{V(\tilde{\Omega}_h;\tilde{\mathcal{T}}_h)} = \|v_h\|_a$ for all $v_h \in V_h$, thanks to the property $|v_h|_{m+1,T} = 0$ for all $T \in \tilde{\mathcal{T}}_h$. Note as well that $H^{m+1}(\tilde{\Omega}_h) \subset V(\tilde{\Omega}_h; \tilde{\mathcal{T}}_h)$.

Property 1. *There exists a constant $C_D > 0$ independent of h such that*

$$\|h^{i-1/2}\, \mathcal{D}^i_{\boldsymbol{d}}\, w\|_{0;\tilde{\Gamma}_{D,h}} \leq C_D\, \|w\|_{V(\tilde{\Omega}_h;\tilde{\mathcal{T}}_h)}\,, \qquad \forall w \in V(\tilde{\Omega}_h; \tilde{\mathcal{T}}_h)\,, \qquad 1 \leq i \leq m\,. \tag{62}$$

Proof. Writing $\boldsymbol{d} = \|\boldsymbol{d}\|\boldsymbol{\nu}$, it holds $\mathcal{D}^i_{\boldsymbol{d}}\, w = \|\boldsymbol{d}\|^i \mathcal{D}^i_{\boldsymbol{\nu}}\, w$, whence by (58) and (61), recalling (5),

$$\|h^{i-1/2}\mathcal{D}^i_{\boldsymbol{d}}\, w\|_{0;\tilde{\Gamma}_{D,h}} \leq \|h^{-1}\boldsymbol{d}\|_{L^\infty(\tilde{\Gamma}_h)}\|h^{i-1/2}\mathcal{D}^i_{\boldsymbol{\nu}}\, w\|_{0;\tilde{\Gamma}_{D,h}} \leq C_D\, \|w\|_{V(\tilde{\Omega}_h;\tilde{\mathcal{T}}_h)}\,. \tag{63}$$

□

Remark 9. *The norm $\|w\|_{V(\tilde\Omega_h;\tilde{\mathscr{T}}_h)}$ uniformly controls from above the standard norm $\|w\|_{1,\tilde\Omega_h}$. Indeed, the latter is equivalent to the norm $\left(\|\nabla w\|^2_{0,\tilde\Omega_h} + \|w\|^2_{0,\tilde\Gamma_h}\right)^{1/2}$ and one has by Property 1 with $i = 1$*

$$\|w\|_{0,\tilde\Gamma_h} \lesssim \|h^{-1/2} w\|_{0,\tilde\Gamma_h} \leq \|h^{-1/2} S^1_h w\|_{0,\tilde\Gamma_h} + \|h^{-1/2}\,\mathscr{D}_{\boldsymbol{d}}\, w\|_{0,\tilde\Gamma_h} \lesssim \|w\|_{V(\tilde\Omega_h;\tilde{\mathscr{T}}_h)}\,. \tag{64}$$

Theorem 3 (Continuity, Poisson)**.** *The bilinear form a_h introduced in* (15) *is defined in $V(\tilde\Omega_h;\tilde{\mathscr{T}}_h) \times V(\tilde\Omega_h;\tilde{\mathscr{T}}_h)$ and uniformly continuous therein; precisely, there exists $A > 0$ independent of h such that*

$$|\, a_h(w, v)\,| \leq A\, \|w\|_{V(\tilde\Omega_h;\tilde{\mathscr{T}}_h)}\, \|v\|_{V(\tilde\Omega_h;\tilde{\mathscr{T}}_h)}\,, \qquad \forall w, v \in V(\tilde\Omega_h;\tilde{\mathscr{T}}_h)\,. \tag{65}$$

Proof. The proof exploits Property 1, with arguments similar to those detailed in the proof of the following Theorem 4. □

6.2. Stokes problem

We now turn to discuss the continuity of the form $\mathscr{B}_h$. To this end, we define the following spaces.

Definition 2. *Let $V(\tilde\Omega_h;\tilde{\mathscr{T}}_h) = V(\tilde\Omega_h;\tilde{\mathscr{T}}_h, m)$ be defined in* (60)*. Then, let us set*

$$\boldsymbol{V}(\tilde\Omega_h;\tilde{\mathscr{T}}_h) = \boldsymbol{V}(\tilde\Omega_h;\tilde{\mathscr{T}}_h, m) := (V(\tilde\Omega_h;\tilde{\mathscr{T}}_h, m) \cap H^2(\tilde\Omega_h;\tilde{\mathscr{T}}_h))^n\,, \tag{66}$$

(where $H^2(\tilde\Omega_h;\tilde{\mathscr{T}}_h) := \{v \in H^1(\tilde\Omega_h) : v_{|T} \in H^2(T)\ \forall T \in \tilde{\mathscr{T}}_h\}$) and

$$Q(\tilde\Omega_h) = \begin{cases} H^1(\tilde\Omega_h) & \text{if } \Gamma_N \neq \emptyset \\ H^1(\tilde\Omega_h) \cap L^2_0(\tilde\Omega_h) & \text{otherwise} \end{cases} \tag{67}$$

Furthermore, let us define $\boldsymbol{W}(\tilde\Omega_h;\tilde{\mathscr{T}}_h) = \boldsymbol{V}(\tilde\Omega_h;\tilde{\mathscr{T}}_h) \times Q(\tilde\Omega_h)$, equipped with the norm

$$\|\,[\boldsymbol{v}, q]\|^2_{\boldsymbol{W}(\tilde\Omega_h;\tilde{\mathscr{T}}_h)} := \|\,[\boldsymbol{v}, q]\,\|^2_{\mathscr{B}} + 2\mu\, |h^m\, \boldsymbol{v}|^2_{m+1,\tilde{\mathscr{T}}^b_h} + 2\mu\, |h\, \boldsymbol{v}|^2_{2,\tilde\Omega_h,\tilde{\mathscr{T}}_h}\,. \tag{68}$$

Note that $\boldsymbol{W}_h \subset \boldsymbol{W}(\tilde\Omega_h;\tilde{\mathscr{T}}_h)$ and that there exists $C > 0$ independent of h such that $\|[\boldsymbol{v}_h, q_h]\|_{\boldsymbol{W}(\tilde\Omega_h;\tilde{\mathscr{T}}_h)} \leq C\,\|\,[\boldsymbol{v}_h, q_h]\,\|_{\mathscr{B}}$ for all $[\boldsymbol{v}_h, q_h] \in \boldsymbol{W}_h$. Finally, recalling Remark 9, the norm $\|\boldsymbol{v}\|_{V(\tilde\Omega_h;\tilde{\mathscr{T}}_h)}$ uniformly controls from above the standard norm $\|\boldsymbol{v}\|_{1,\tilde\Omega_h}$.

The following property is the counterpart of Property 1.

Property 2. *There exists a constant $C_D > 0$ independent of h such that*

$$\|(2\mu)^{1/2} h^{i-1/2}\, \mathscr{D}^i_{\boldsymbol{d}}\, \boldsymbol{w}\|_{0;\tilde\Gamma_{D,h}} \leq C_D\, \|\boldsymbol{w}\|_{V(\tilde\Omega_h;\tilde{\mathscr{T}}_h)}\,, \qquad \forall \boldsymbol{w} \in \boldsymbol{V}(\tilde\Omega_h;\tilde{\mathscr{T}}_h)\,, \qquad 1 \leq i \leq m\,. \tag{69}$$

Theorem 4 (Continuity, Stokes)**.** *The bilinear form $\mathscr{B}_h$ introduced in* (22a) *is defined in $\boldsymbol{W}(\tilde\Omega_h;\tilde{\mathscr{T}}_h) \times \boldsymbol{W}_h(\tilde\Omega_h;\tilde{\mathscr{T}}_h)$ and uniformly continuous therein; precisely, there exists $C_{\mathscr{B}} > 0$ independent of h such that*

$$|\,\mathscr{B}_h([\boldsymbol{u}, p], [\boldsymbol{w}_h, q_h])\,| \leq C_{\mathscr{B}}\, \|\,[\boldsymbol{u}, p]\,\|_{\boldsymbol{W}(\tilde\Omega_h;\tilde{\mathscr{T}}_h)}\, \|\,[\boldsymbol{w}_h, q_h]\,\|_{\mathscr{B}}\,, \tag{70}$$

$\forall [\boldsymbol{u}, p] \in \boldsymbol{W}(\tilde\Omega_h;\tilde{\mathscr{T}}_h)$ and $\forall [\boldsymbol{w}_h, q_h] \in \boldsymbol{W}_h(\tilde\Omega_h;\tilde{\mathscr{T}}_h)$.

Proof. For convenience, we add and subtract the terms $((\nabla \boldsymbol{w}_h)\boldsymbol{d}, 2\,\mu\,\boldsymbol{\varepsilon}(\boldsymbol{u})\tilde{\boldsymbol{n}})_{\tilde\Gamma_{D,h}}$ and $((\nabla \boldsymbol{w}_h)\boldsymbol{d}, p\,\tilde{\boldsymbol{n}})_{\tilde\Gamma_{D,h}}$ to the bilinear form $\mathscr{B}_h([\boldsymbol{u}, p]; [\boldsymbol{w}_h, q_h])$ and obtain:

$$\begin{aligned}\mathscr{B}_h([\boldsymbol{u}, p]; [\boldsymbol{w}_h, q_h]) = {}& (2\,\mu\,\boldsymbol{\varepsilon}(\boldsymbol{u}), \boldsymbol{\varepsilon}(\boldsymbol{w}_h))_{0,\tilde\Omega_h} - (p, \nabla\cdot\boldsymbol{w}_h)_{0,\tilde\Omega_h} + (\nabla\cdot\boldsymbol{u}, q_h)_{0,\tilde\Omega_h} - (2\,\mu\,\boldsymbol{\varepsilon}(\boldsymbol{u})\tilde{\boldsymbol{n}}, \boldsymbol{S}^1_h \boldsymbol{w}_h)_{0,\tilde\Gamma_{D,h}} + (p\,\tilde{\boldsymbol{n}}, \boldsymbol{S}^1_h \boldsymbol{w}_h)_{0,\tilde\Gamma_{D,h}} \\ & + ((\nabla \boldsymbol{w}_h)\boldsymbol{d}, 2\,\mu\,\boldsymbol{\varepsilon}(\boldsymbol{u})\tilde{\boldsymbol{n}})_{0,\tilde\Gamma_{D,h}} - ((\nabla \boldsymbol{w}_h)\boldsymbol{d}, p\,\tilde{\boldsymbol{n}})_{0,\tilde\Gamma_{D,h}} - (\boldsymbol{S}^m_h \boldsymbol{u} \otimes \tilde{\boldsymbol{n}}, 2\,\mu\,\boldsymbol{\varepsilon}(\boldsymbol{w}_h) + q_h \boldsymbol{I})_{0,\tilde\Gamma_{D,h}}\end{aligned}$$

$$
\begin{aligned}
&+ \gamma\,(2\,\mu\, h_\perp^{-1} \boldsymbol{S}_h^m \boldsymbol{u}, \boldsymbol{S}_h^1 \boldsymbol{w}_h)_{0,\tilde\Gamma_{D,h}} + \delta \sum_{T\in\tilde{\mathscr{T}}_h} \Big(h_\tau^2 (2\,\mu)^{-1}(-\nabla\cdot(2\,\mu\,\boldsymbol{\varepsilon}(\boldsymbol{u})) + \nabla p), \nabla q_h \Big)_{0,T} \\
\le\; & \|(2\,\mu)^{1/2}\boldsymbol{\varepsilon}(\boldsymbol{u})\|_{0;\tilde\Omega_h} \|(2\,\mu)^{1/2}\boldsymbol{\varepsilon}(\boldsymbol{w}_h)\|_{0;\tilde\Omega_h} + \|(2\,\mu)^{-1/2} p\|_{0;\tilde\Omega_h} \|(2\,\mu)^{1/2}\nabla\cdot\boldsymbol{w}_h\|_{0;\tilde\Omega_h} \\
&+ \|(2\,\mu)^{1/2}\nabla\cdot\boldsymbol{u}\|_{0;\tilde\Omega_h} \|(2\,\mu)^{-1/2} q_h\|_{0;\tilde\Omega_h} + \|(2\,\mu\, h)^{1/2}\boldsymbol{\varepsilon}(\boldsymbol{u})\|_{0;\tilde\Gamma_{D,h}} \|(2\,\mu)^{1/2} h^{-1/2} \boldsymbol{S}_h^1 \boldsymbol{w}_h\|_{0;\tilde\Gamma_{D,h}} \\
&+ \|(2\,\mu)^{-1/2} h^{1/2} p\|_{0;\tilde\Gamma_{D,h}} \|(2\,\mu)^{1/2} h^{-1/2} \boldsymbol{S}_h^1 \boldsymbol{w}_h\|_{0;\tilde\Gamma_{D,h}} \\
&+ \|h^{-1}\boldsymbol{d}\|_{L^\infty(\tilde\Gamma_h)} \|(2\,\mu)^{1/2} h^{1/2} \boldsymbol{\varepsilon}(\boldsymbol{u})\|_{0;\tilde\Gamma_{D,h}} \|(2\,\mu)^{1/2} h^{1/2} \nabla \boldsymbol{w}_h\|_{0;\tilde\Gamma_{D,h}} \\
&+ \|h^{-1}\boldsymbol{d}\|_{L^\infty(\tilde\Gamma_h)} \|(2\,\mu)^{-1/2} h^{1/2} p\|_{0;\tilde\Gamma_{D,h}} \|(2\,\mu)^{1/2} h^{1/2} \nabla \boldsymbol{w}_h\|_{0;\tilde\Gamma_{D,h}} \\
&+ \|(2\,\mu)^{1/2} h^{-1/2} \boldsymbol{S}_h^1 \boldsymbol{u}\|_{0;\tilde\Gamma_{D,h}} \|(2\,\mu)^{1/2} h^{1/2} \boldsymbol{\varepsilon}(\boldsymbol{w}_h)\|_{0;\tilde\Gamma_{D,h}} + \|(2\,\mu)^{1/2} h^{-1/2} \boldsymbol{S}_h^1 \boldsymbol{u}\|_{0;\tilde\Gamma_{D,h}} \|(2\,\mu)^{-1/2} h^{1/2} q_h\|_{0;\tilde\Gamma_{D,h}} \\
&+ \left(\sum_{i=2}^m \frac{\|h^{-1}\boldsymbol{d}\|^i_{L^\infty(\tilde\Gamma_h)}}{i!} \|(2\mu)^{1/2} h^{i-1/2} \mathscr{D}^i_{\boldsymbol{d}} \boldsymbol{u}\|_{0;\tilde\Gamma_{D,h}} \right) \|(2\,\mu)^{1/2} h^{1/2} \boldsymbol{\varepsilon}(\boldsymbol{w}_h)\|_{0;\tilde\Gamma_{D,h}} \\
&+ \left(\sum_{i=2}^m \frac{\|h^{-1}\boldsymbol{d}\|^i_{L^\infty(\tilde\Gamma_h)}}{i!} \|(2\mu)^{1/2} h^{i-1/2} \mathscr{D}^i_{\boldsymbol{d}} \boldsymbol{u}\|_{0;\tilde\Gamma_{D,h}} \right) \|(2\,\mu)^{-1/2} h^{1/2} q_h\|_{0;\tilde\Gamma_{D,h}} \\
&+ \gamma \|(2\,\mu)^{1/2} h^{-1/2} \boldsymbol{S}_h^1 \boldsymbol{u}\|_{0;\tilde\Gamma_{D,h}} \|(2\,\mu)^{1/2} h^{-1/2} \boldsymbol{S}_h^1 \boldsymbol{w}_h\|_{0;\tilde\Gamma_{D,h}} \\
&+ \gamma \left(\sum_{i=2}^m \frac{\|h^{-1}\boldsymbol{d}\|^i_{L^\infty(\tilde\Gamma_h)}}{i!} \|(2\mu)^{1/2} h^{i-1/2} \mathscr{D}^i_{\boldsymbol{d}} \boldsymbol{u}\|_{0;\tilde\Gamma_{D,h}} \right) \|(2\,\mu)^{1/2} h^{-1/2} \boldsymbol{S}_h^1 \boldsymbol{w}_h\|_{0;\tilde\Gamma_{D,h}} \\
&+ \delta\, \|(2\,\mu)^{-1/2} h\, \nabla p\|_{0;\tilde\Omega_h} \|(2\,\mu)^{-1/2} h\, \nabla q_h\|_{0;\tilde\Omega_h} \\
&+ \delta\, \|(2\,\mu)^{1/2} h\, \nabla\cdot\boldsymbol{\varepsilon}(\boldsymbol{u})\|_{0;\tilde\Omega_h;\mathscr{T}^h} \|(2\,\mu)^{-1/2} h\, \nabla q_h\|_{0;\tilde\Omega_h}\,.
\end{aligned} \tag{71}
$$

Using Properties 3 and 4 in the Appendix and Property 2 above, along with the fact that $\|\nabla\cdot\boldsymbol{\epsilon}(\boldsymbol{u})\|_{0;\tilde\Omega_h;\mathscr{T}^h} \lesssim \|\nabla\boldsymbol{\varepsilon}(\boldsymbol{u})\|_{0;\tilde\Omega_h;\mathscr{T}^h} \le \|\Delta\boldsymbol{u}\|_{0;\tilde\Omega_h;\mathscr{T}^h}$ and $\|\nabla\cdot\boldsymbol{u}\|_{0;\tilde\Omega_h} \lesssim \|\nabla\boldsymbol{u}\|_{0;\tilde\Omega_h}$, after some tedious algebra we obtain the desired result. $\square$

7. Analysis of the Taylor remainder

This section is devoted to the analysis of the behavior of the Taylor remainder $R_h^m u = \bar g - S_h^m u$ in the expansion of u on $\tilde\Gamma_h$, introduced in (7). In particular, we are interested in estimating a weighted L^2-norm of $R_h^m u$ along $\tilde\Gamma_h$ in terms of the mesh parameter h_Γ. We detail our analysis for the two-dimensional situation, since the extension to three dimensions poses no difficulties.

Let $\tilde E \subset \tilde\Gamma_h$ be an edge of a triangle $T = T_{\tilde E} \in \tilde{\mathscr{T}}_h^b$ such that $\boldsymbol{M}_h(\tilde E) \subset \Gamma_D$. Since $\boldsymbol{x} = \boldsymbol{M}_h(\tilde{\boldsymbol{x}})$ is the closest-point projection upon Γ for all $\tilde{\boldsymbol{x}} \in \tilde E$, the vector $\boldsymbol{d}(\tilde{\boldsymbol{x}})$ is aligned with the unit outward normal vector $\boldsymbol{n}(\boldsymbol{x})$ to Γ. Let $\tilde{\boldsymbol{x}}_a$, $\tilde{\boldsymbol{x}}_b$ be the endpoints of $\tilde E$, and $h_E := \|\tilde{\boldsymbol{x}}_b - \tilde{\boldsymbol{x}}_a\|$ its length. Introducing the unit vector $\tilde{z} := h_{\tilde E}^{-1}(\tilde{\boldsymbol{x}}_b - \tilde{\boldsymbol{x}}_a)$, let us parametrize the points in $\tilde E$ by $\tilde{\boldsymbol{x}}(\tau) = \tilde{\boldsymbol{x}}_a + \tau\tilde{z}$ with $0 \le \tau \le h_{\tilde E}$. Correspondingly, points in $\boldsymbol{M}_h(\tilde E)$ are parametrized by $\boldsymbol{x}(\tau) = \boldsymbol{M}_h(\tilde{\boldsymbol{x}}(\tau))$; let us set $\boldsymbol{n}(\tau) := \boldsymbol{n}(\boldsymbol{x}(\tau))$. Furthermore, let us introduce the 2D parametrization

$$
\boldsymbol{x}(\tau,\sigma) = \boldsymbol{\Phi}(\tau,\sigma) := \tilde{\boldsymbol{x}}(\tau) + \sigma\boldsymbol{n}(\tau)\,, \qquad 0 \le \tau \le h_{\tilde E}, \quad 0 \le \sigma \le d(\tau) := \|\boldsymbol{d}(\tilde{\boldsymbol{x}}(\tau))\|\,, \tag{72}
$$

as shown in Figure 2. Note that $\boldsymbol{\Phi}$ takes values in $\bar\Omega$, and satisfies $\boldsymbol{\Phi}(\tau, d(\tau)) = \boldsymbol{x}(\tau)$ for $0 \le \tau \le h_{\tilde E}$. In order to compute the remainder $R_h^m u$ at the point $\tilde{\boldsymbol{x}}(\tau)$ for some fixed τ, let us introduce the mapping $\phi(\sigma) := u(\boldsymbol{\Phi}(\tau,\sigma))$. Then, assuming u smooth enough (or applying a density argument), one has the Taylor representation

$$
\bar g(\tilde{\boldsymbol{x}}(\tau)) = \phi(d(\tau)) = \phi(0) + \frac{\mathrm{d}\phi}{\mathrm{d}\sigma}(0) d(\tau) + \ldots + \int_0^{d(\tau)} \frac{\mathrm{d}^{m+1}\phi}{\mathrm{d}\sigma^{m+1}}(s) \frac{(d(\tau)-s)^m}{m!}\,\mathrm{d}s\,,
$$

with

$$
\phi(0) = u(\tilde{\boldsymbol{x}}(\tau))\,, \quad \frac{\mathrm{d}\phi}{\mathrm{d}\sigma}(0) = \nabla u(\tilde{\boldsymbol{x}}(\tau))\cdot\boldsymbol{n}(\tau)\,, \quad \frac{\mathrm{d}^{m+1}\phi}{\mathrm{d}\sigma^{m+1}}(s) = \mathscr{D}^{m+1}_{\boldsymbol{n}(\tau)} u(\boldsymbol{x}(\tau,\sigma))\,.
$$

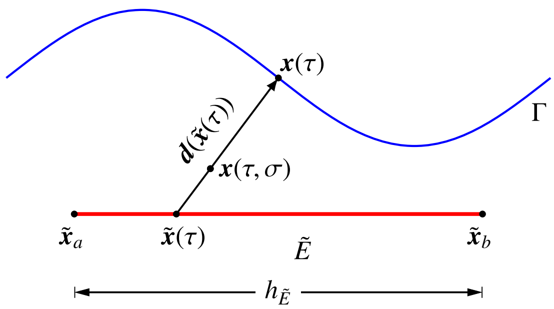

Figure 2: Representation of a portion of the boundary Γ, a surrogate edge $\tilde{E}$ and their respective parametrization.

It follows that

$$(R_h^m u)(\tilde{\boldsymbol{x}}(\tau)) = \int_0^{d(\tau)} \mathscr{D}_{\boldsymbol{n}(\tau)}^{m+1} u(\boldsymbol{x}(\tau,s)) \frac{(d(\tau)-s)^m}{m!} \, \mathrm{d}s \,. \tag{73}$$

Using Hölder's inequality for $\frac{1}{p}+\frac{1}{q}=1$ with $2 \le p \le \infty$, we easily get

$$|(R_h^m u)(\tilde{\boldsymbol{x}}(\tau))| \le \frac{1}{m!(1+mq)^{1/q}} (d(\tau))^{m+1/q} \left(\int_0^{d(\tau)} \|\mathscr{D}^{m+1} u(\boldsymbol{x}(\tau,s))\|^p \, \mathrm{d}s \right)^{1/p} .$$

Squaring and integrating over $\tilde{E}$, and using once more Hölder's inequality, we get, with $d_{\tilde{E}} := \max_{\tau \in [0,h_{\tilde{E}}]} d(\tau)$,

$$\|R_h^m u\|_{0,\tilde{E}}^2 \le c_p \, d_{\tilde{E}}^{2(m+1-1/p)} h_{\tilde{E}}^{1-2/p} \left(\int_0^{h_{\tilde{E}}} \int_0^{d(\tau)} \|\mathscr{D}^{m+1} u(\boldsymbol{x}(\tau,s))\|^p \, \mathrm{d}s \, \mathrm{d}\tau \right)^{2/p} . \tag{74}$$

Now, define the region $\mathscr{R}_{\tilde{E}} := \{(\tau,\sigma) : 0 \le \tau \le h_{\tilde{E}}, \ 0 \le \sigma \le d(\tau)\}$ and set $\mathscr{A}_{\tilde{E}} := \boldsymbol{\Phi}(\mathscr{R}_{\tilde{E}}) \subset \bar{\Omega}$. We proceed in two different ways, depending on the fulfillment of the following *non-orthogonality condition*: there exists a constant $\varrho > 0$ independent of h such that

$$|(\tilde{\boldsymbol{n}} \cdot \boldsymbol{\nu})(\tilde{\boldsymbol{x}})| \ge \varrho \,, \qquad \forall \tilde{\boldsymbol{x}} \in T \cap \tilde{\Gamma}_h \,, \quad \forall T \in \tilde{\mathscr{T}}_h \,, \tag{75}$$

where $\tilde{\boldsymbol{n}}$ is the unit normal vector to the surrogate boundary $\tilde{\Gamma}_h$, and $\boldsymbol{\nu}$ is the unit vector aligned with the distance $\boldsymbol{d}$.

Remark 10. *Assumption 2 or 3 for the Poisson or Stokes problems, respectively, imply* (75). *In fact, if an edge $E \subset T$ on the surrogate boundary is orthogonal to the true boundary, there will be points on that edge with a distance from the true boundary larger than or equal to the length $|E|$ of the edge; since $|E| \ge c\, h_T$ for some constant $c \in (0,1)$ depending on the regularity of the mesh, for these points one has $\|h_T^{-1} \boldsymbol{d}\| \ge c$, which contradicts Assumption 2 (Assumption 3, resp.) if β (χ, resp.) is chosen small enough.*

If the condition (75) is satisfied, then one can prove (see e.g., [2, Lemma 1] or [48, Lemma 3.4]) that there exists a constant $b > 0$ independent of $\tilde{E}$ such that for $h_{\tilde{E}}$ small enough the Jacobian matrix $\boldsymbol{J\Phi}$ of the mapping (72) satisfies

$$|\det \boldsymbol{J\Phi}(\tau,\sigma)| \ge b \,, \qquad \forall (\tau,\sigma) \in \mathscr{R}_{\tilde{E}} \,.$$

This allows us to apply a change of variable in the previous integral. Precisely, if $u \in H^{m+1}(\mathscr{A}_{\tilde{E}})$ one has

$$\int_0^{h_{\tilde{E}}} \int_0^{d(\tau)} \|\mathscr{D}^{m+1} u(\boldsymbol{x}(\tau,s))\|^2 \, \mathrm{d}s \, \mathrm{d}\tau \le \frac{1}{b} \int_{\mathscr{A}_{\tilde{E}}} \|\mathscr{D}^{m+1} u(\boldsymbol{x}(\tau,s))\|^2 \, \mathrm{d}\boldsymbol{x} \,.$$

Thus, from (74) (with $p=2$) and (5), we derive the existence of a constant $\bar{c}_2 > 0$ independent of $\tilde{E}$ such that

$$\|h_{\tilde{E}}^{-1/2} R_h^m u\|_{0,\tilde{E}}^2 \le \bar{c}_2 h_{\tilde{E}}^{2m} |u|_{m+1,\mathscr{A}_{\tilde{E}}}^2 \,. \tag{76}$$

Let Ω_S be a neighborhood of Γ in $\bar{\Omega}$ satisfying

$$\bigcup_{\tilde{E}\subset\tilde{\Gamma}_h} \mathscr{A}_{\tilde{E}} \subseteq \Omega_S \,. \tag{77}$$

Note that the sets $\mathscr{A}_{\tilde{E}}$ may overlap only a number of times bounded independently of the meshsize. Hence, if $u \in H^{m+1}(\Omega_S)$, we obtain

$$\|h^{-1/2} R_h^m u\|^2_{0,\tilde{\Gamma}_h} \leq \bar{c}_2 \, h_\Gamma^{2m} \sum_{\tilde{E}\subset\tilde{\Gamma}_h} |u|^2_{m+1,\mathscr{A}_{\tilde{E}}} \leq C_2 \, h_\Gamma^{2m} |u|^2_{m+1,\Omega_S} \,.$$

Suppose now that condition (75) is not satisfied. In this case, we may assume the stronger smoothness condition $u \in C^{m+1}(\overline{\mathscr{A}}_{\tilde{E}})$; going back to inequality (74) with $p = \infty$, we can replace (76) by the following bound

$$\|h_{\tilde{E}}^{-1/2} R_h^m u\|^2_{0,\tilde{E}} \leq \bar{c}_\infty h_{\tilde{E}}^{2(m+1)} |u|^2_{C^{m+1}(\overline{\mathscr{A}}_{\tilde{E}})} \tag{78}$$

and proceed as above.

Summarizing, we have obtained the following result.

Proposition 2. *Let Ω_S satisfy* (77). *i) If condition* (75) *holds, and the exact solution satisfies $u \in H^{m+1}(\Omega_S)$, there exists a constant $C_2 > 0$ independent of h_Γ such that*

$$\|h^{-1/2} R_h^m u\|_{0,\tilde{\Gamma}_h} \leq C_2 \, h_\Gamma^m \, |u|_{m+1,\Omega_S} \,. \tag{79}$$

ii) If condition (75) *does not hold, but the exact solution satisfies $u \in C^{m+1}(\overline{\Omega_S})$, there exists a constant $\bar{C}_\infty > 0$ independent of h_Γ such that*

$$\|h^{-1/2} R_h^m u\|_{0,\tilde{\Gamma}_h} \leq \bar{C}_\infty \, h_\Gamma^{m+1/2} |u|_{C^{m+1}(\overline{\Omega_S})} \,. \tag{80}$$

Remark 11. *From Proposition 2 one can immediately obtain analogous estimates for the remainder of the Taylor expansion of the solution **u** of the Stokes problem.*

8. Consistency and convergence in the energy norm

The results given in this section extend in a rather straightforward manner those for the low-order case $m = 1$, available in [2, 4]; for this reason, we just highlight the main steps. The analysis hinges upon Strang's Second Lemma: the approximation error is bounded using classical results in finite elements, whereas the consistency error is controlled by the estimate on the Taylor remainder given in the previous section.

8.1. Poisson problem

Strang's Lemma reads

$$\|u - u_h\|_{V(\tilde{\Omega}_h;\tilde{\mathscr{T}}_h)} \leq \left(1 + \alpha^{-1} A\right) E_{a,h}(u) + \alpha^{-1} E_{c,h}(u) \,, \tag{81}$$

where the approximation error and the consistency error are defined by

$$E_{a,h}(u) := \inf_{v_h\in V_h} \|u - v_h\|_{V(\tilde{\Omega}_h;\tilde{\mathscr{T}}_h)} \,, \qquad E_{c,h}(u) := \sup_{v_h\in V_h} \frac{a_h(u, v_h) - \ell_h(v_h)}{\|v_h\|_{V(\tilde{\Omega}_h;\tilde{\mathscr{T}}_h)}} \,. \tag{82}$$

They can be estimated as indicated in the following propositions, whose proofs are omitted since they are similar to those for the analogous results given below for the Stokes problem.

Proposition 3. *Let $u \in H^{m+1}(\Omega)$. There exists a constant $C_a > 0$ independent of u and the meshsize such that*

$$E_{a,h}(u) \leq C_a h_\Omega^m \, |u|_{m+1,\tilde{\Omega}_h} \,. \tag{83}$$

We estimate the consistency error $E_{c,h}(u)$ using Proposition 2 and the identity $a_h(u, v_h) - \ell_h(v_h) = (R_h^m u, \partial_{\tilde{n}} v_h)_{0,\tilde{\Gamma}_h} + \gamma \, (h^{-1} R_h^m u, S_h^1 v_h)_{0,\tilde{\Gamma}_h}$.

Proposition 4. *Let $u \in H^{m+1}(\Omega)$. If condition* (75) *holds true, there exists a constant $C_c > 0$ independent of u and the meshsize such that*

$$E_{c,h}(u) \le C_c\, h_\Gamma^m |u|_{m+1,\Omega_S} \,. \tag{84}$$

If condition (75) *does not hold but $u \in C^{m+1}(\overline{\Omega_S})$, there exists a constant $C_c > 0$ independent of u and the meshsize such that*

$$E_{c,h}(u) \le C_c\, h_\Gamma^{m+1/2} |u|_{C^{m+1}(\overline{\Omega_S})} \,. \tag{85}$$

Based on the latter result, we formulate the following regularity requirement on the exact solution u.

Assumption 4. *Let $u \in H^{m+1}(\Omega)$. In addition, either i) condition* (75) *holds true, or ii) condition* (75) *does not hold but $u \in C^{m+1}(\overline{\Omega_S})$.*

Consequently, it is convenient to define the seminorm

$$|u|_{m+1,\star} = \begin{cases} |u|_{m+1,\Omega} & \text{in case } i)\,, \\ |u|_{m+1,\tilde{\Omega}_h} + h_\Gamma^{1/2}\, |u|_{C^{m+1}(\overline{\Omega_S})} & \text{in case } ii)\,. \end{cases} \tag{86}$$

Then, we obtain an estimate of the discretization error $u - u_h$ in the 'energy' norm by substituting (83) and (84) in (81), together with the inequality $h_\Gamma \le h_\Omega$.

Theorem 5. *Under Assumption 4 and the hypotheses made in Theorem 1, there exists a constant $C > 0$ independent of u and the meshsize such that*

$$\|u - u_h\|_{V(\tilde{\Omega}_h;\tilde{\mathcal{T}}_h)} \le C\, h_\Omega^m\, |u|_{m+1,\star} \,. \tag{87}$$

8.2. Stokes problem

Strang Lemma now reads

$$|||[\boldsymbol{u}, p] - [\boldsymbol{u}_h, p_h]|||_{\boldsymbol{W}(\tilde{\Omega}_h;\tilde{\mathcal{T}}_h)} \le \left(1 + \alpha_{LBB}^{-1} \|\mathscr{B}\|_{\boldsymbol{W}(\tilde{\Omega}_h;\tilde{\mathcal{T}}_h)\times \boldsymbol{W}_h(\tilde{\Omega}_h;\tilde{\mathcal{T}}_h)}\right) E_{\mathscr{B},a,h}([\boldsymbol{u}, p]) + \alpha_{LBB}^{-1} E_{\mathscr{B},c,h}([\boldsymbol{u}, p]) \tag{88a}$$

with

$$E_{\mathscr{B},a,h}([\boldsymbol{u}, p]) := \inf_{[\boldsymbol{w}_h, q_h] \in \boldsymbol{W}_h(\tilde{\Omega}_h;\tilde{\mathcal{T}}_h)} |||[\boldsymbol{u}, p] - [\boldsymbol{w}_h, q_h]|||_{\boldsymbol{W}(\tilde{\Omega}_h;\tilde{\mathcal{T}}_h)} \,, \tag{88b}$$

$$E_{\mathscr{B},c,h}([\boldsymbol{u}, p]) := \sup_{[\boldsymbol{w}_h, q_h] \in \boldsymbol{W}_h(\tilde{\Omega}_h;\tilde{\mathcal{T}}_h)} \frac{|\mathscr{L}_h([\boldsymbol{w}_h, q_h]) - \mathscr{B}_h([\boldsymbol{u}, p]; [\boldsymbol{w}_h, q_h])|}{|||[\boldsymbol{w}_h, q_h]|||_{\boldsymbol{W}(\tilde{\Omega}_h;\tilde{\mathcal{T}}_h)}} \,. \tag{88c}$$

We are going to estimate both errors in terms of the meshsize h_Ω introduced in (2).

Proposition 5. *Let $\boldsymbol{u} \in (H^{m+1}(\Omega))^n$ and $p \in H^m(\Omega)$. There exists a constant $C_{APP} > 0$ independent of $[\boldsymbol{u}, p]$ and the mesh size such that*

$$E_{\mathscr{B},a,h}([\boldsymbol{u}, p]) \le C_{APP}\, h_\Omega^m \left(\mu^{1/2} |\boldsymbol{u}|_{m+1;\tilde{\Omega}_h} + \mu^{-1/2} |p|_{m;\tilde{\Omega}_h}\right) \,. \tag{89}$$

Proof. Since $H^r(\Omega) \subset C^0(\bar{\Omega})$ with continuous injection for $r \ge 2$, we can set $\boldsymbol{w}_h = I_h^m \boldsymbol{u}$ where $I_h^m \boldsymbol{u}$ is the globally continuous, m-th order piecewise polynomial interpolant at the nodes of $\tilde{\mathcal{T}}_h$. Also, we set $q_h = I_h^m p$ if $m \ge 2$, or $q_h = I_h^{SZ} p$ for $m = 1$ (where I_h^{SZ} is the piecewise linear Scott-Zhang interpolant on the same grid), corrected by an additive constant to satisfy the zero-average condition in the pure Dirichlet case. We can now estimate the interpolation error $|||[\boldsymbol{e}_{\boldsymbol{u}}^I, e_p^I]|||_{\boldsymbol{W}(\tilde{\Omega}_h;\tilde{\mathcal{T}}_h)}$ where $\boldsymbol{e}_{\boldsymbol{u}}^I := \boldsymbol{u} - \boldsymbol{w}_h$ and $e_p^I := p - q_h$. Classical approximation results for these operators yield

$$\|(2\mu)^{1/2} \nabla \boldsymbol{e}_{\boldsymbol{u}}^I\|_{0;\tilde{\Omega}_h} + l(\tilde{\Omega}_h)^{-1} \|(2\mu)^{1/2} \boldsymbol{e}_{\boldsymbol{u}}^I\|_{0;\tilde{\Omega}_h} \le C_1\, \mu^{1/2} h_\Omega^m\, |\boldsymbol{u}|_{m+1;\tilde{\Omega}_h} \tag{90a}$$

and

$$\|(2\mu)^{-1/2} e_p^I\|_{0;\tilde{\Omega}_h} + \|(2\mu)^{-1/2} h\, \nabla e_p^I\|_{0;\tilde{\Omega}_h} \le C_2\, \mu^{-1/2} h_\Omega^m\, |p|_{m;\tilde{\Omega}_h} \,. \tag{90b}$$

On the other hand,

$$\|(2\mu)^{1/2}h^{-1/2}\boldsymbol{S}_h^1\boldsymbol{e}_{\boldsymbol{u}}^I\|_{0;\tilde{\Gamma}_{D,h}} \le \|(2\mu)^{1/2}h^{-1/2}\boldsymbol{e}_{\boldsymbol{u}}^I\|_{0;\tilde{\Gamma}_{D,h}} + \|(2\mu)^{1/2}h^{-1/2}(\nabla\boldsymbol{e}_{\boldsymbol{u}}^I)\boldsymbol{d}\|_{0;\tilde{\Gamma}_{D,h}} \,. \tag{91}$$

Using (58) and (5) to bound the norms on the right-hand side, we obtain

$$\|(2\mu)^{1/2}h^{-1/2}\boldsymbol{S}_h^1\boldsymbol{e}_{\boldsymbol{u}}^I\|_{0;\tilde{\Gamma}_{D,h}} \le\; c\,\mu^{1/2}\left(\|h^{-1}\boldsymbol{e}_{\boldsymbol{u}}^I\|_{0;\tilde{\mathscr{T}}_h^b} + |\boldsymbol{e}_{\boldsymbol{u}}^I|_{1;2;\tilde{\Omega}_h^b} + |h\,\boldsymbol{e}_{\boldsymbol{u}}^I|_{2;\tilde{\mathscr{T}}_h^b}\right) \le\; C_3\,\mu^{1/2}h_\Omega^m|\boldsymbol{u}|_{m+1;\tilde{\Omega}_h^b}\,. \tag{92}$$

We conclude by observing that the remaining norms in (68) can be bounded in a similar way. □

Proposition 6. *Let* $\boldsymbol{u} \in (H^{m+1}(\Omega))^n$*. If condition* (75) *holds true, there exists a constant* $C_c > 0$ *independent of* u *and the meshsize such that*

$$E_{\mathscr{B},c,h}([\boldsymbol{u},p]) \le C_c\,\mu^{1/2}h_\Gamma^m\,|\boldsymbol{u}|_{m+1;\Omega_S}\,. \tag{93}$$

If condition (75) *does not hold but* $\boldsymbol{u} \in (C^{m+1}(\overline{\Omega_S}))^n$*, there exists a constant* $C_c > 0$ *independent of* u *and the meshsize such that*

$$E_{\mathscr{B},c,h}([\boldsymbol{u},p]) \le C_c\,\mu^{1/2}h_\Gamma^{m+1/2}|\boldsymbol{u}|_{(C^{m+1}(\overline{\Omega_S}))^n}\,. \tag{94}$$

Proof. By integration by parts and application of Property 3 in the Appendix, one gets for all $[\boldsymbol{w}_h, q_h] \in \boldsymbol{W}_h$

$$\begin{aligned}
\mathscr{L}_h([\boldsymbol{w}_h,q_h]) - \mathscr{B}_h([\boldsymbol{u},p];[\boldsymbol{w}_h,q_h]) &= ((\boldsymbol{S}_h^m\boldsymbol{u}-\bar{\boldsymbol{u}}_D)\otimes\tilde{\boldsymbol{n}}, 2\mu\,\boldsymbol{\varepsilon}(\boldsymbol{w}_h)+q_h\boldsymbol{I})_{0,\tilde{\Gamma}_{D,h}} + \gamma\,(2\mu\,h_\perp^{-1}\left(\boldsymbol{S}_h^m\boldsymbol{u}-\bar{\boldsymbol{u}}_D\right), \boldsymbol{S}_h^1\boldsymbol{w}_h)_{0,\tilde{\Gamma}_{D,h}}\\
&= (R_h^m\boldsymbol{u}\otimes\tilde{\boldsymbol{n}}, 2\mu\,\boldsymbol{\varepsilon}(\boldsymbol{w}_h)+q_h\boldsymbol{I})_{0,\tilde{\Gamma}_{D,h}} + \gamma\,(2\mu\,h_\perp^{-1}R_h^m\boldsymbol{u}, \boldsymbol{S}_h^1\boldsymbol{w}_h)_{0,\tilde{\Gamma}_{D,h}}\\
&\lesssim \|(2\mu)^{1/2}h^{-1/2}R_h^m\boldsymbol{u}\|_{0;\tilde{\Gamma}_{D,h}}\left(\|(2\mu)^{1/2}\nabla\boldsymbol{w}_h\|_{0;\tilde{\Omega}_h^b} + \|(2\mu)^{-1/2}q_h\|_{0;\tilde{\Omega}_h^b}\right.\\
&\qquad \left. + \|(2\mu)^{1/2}h^{-1/2}\boldsymbol{S}_h^1\boldsymbol{w}_h\|_{0;\tilde{\Gamma}_{D,h}}\right),
\end{aligned} \tag{95}$$

whence $E_{\mathscr{B},c,h}([\boldsymbol{u},p]) \le C_{c,1}\|\mu^{1/2}h^{-1/2}R_h^m\boldsymbol{u}\|_{0;\tilde{\Gamma}_{D,h}}$. We conclude using the analogous version of Proposition 2 for vector fields (see Remark 11). □

Combining the two previous properties, we arrive at the following convergence result in the 'energy' norm, which stands as a counterpart of Theorem 5 for the Stokes problem.

Theorem 6. *Let each component of* $\boldsymbol{u}$ *satisfy Assumption 4, and let* $p \in H^m(\Omega)$*. Under the conditions of validity of Theorem 2, there exists a constant* $C > 0$ *independent of* $\boldsymbol{u}$ *and the meshsize such that*

$$\|[\boldsymbol{u},p]-[\boldsymbol{u}_h,p_h]\|_{W(\tilde{\Omega}_h;\tilde{\mathscr{T}}_h)} \le C\,h_\Omega^m\left(\mu^{1/2}|\boldsymbol{u}|_{m+1,\star} + \mu^{-1/2}|p|_{m;\tilde{\Omega}_h}\right)\,. \tag{96}$$

9. Enhanced error estimates in the L^2 norm

In this section, we provide an estimate of the L^2-norm of the discretization error $u - u_h$ (for the Poisson problem), or $\boldsymbol{u} - \boldsymbol{u}_h$ (for the Stokes problem), by adapting to the present setting the classical Aubin-Nitsche duality argument.

9.1. Poisson problem

We begin by strenghtening Assumption 4.

Assumption 5. *Let* $u \in H^{m+1}(\Omega)$*. In addition, let condition* (75) *hold true and let* $u \in W^{m+1,\infty}(\Omega_S)$*.*

Consequently, we can easily improve the result in Proposition 2, by adapting its proof to the new assumption.

Proposition 7. *Under Assumption 5, there exists a constant* $C_\infty > 0$ *independent of* h_Γ *such that*

$$\|h^{-1/2}R_h^m u\|_{0,\tilde{\Gamma}_h} \le C_\infty\,h_\Gamma^{m+1/2}\,|u|_{W^{m+1,\infty}(\Omega_S)}\,. \tag{97}$$

The desired error estimate is as follows.

Theorem 7 (Enhanced L^2-error estimate for u_h)**.** *Under Assumption 5 and the conditions of validity of Theorem 5, there exists a constant $C > 0$ independent of u and the meshsize such that*

$$\|u - u_h\|_{0,\tilde{\Omega}_h} \leq C\, h_\Omega^{m+1/2} \left(|u|_{m+1;\tilde{\Omega}_h} + h_\Omega^{1/2} |u|_{W^{m+1,\infty}(\Omega_S)} \right) . \tag{98}$$

We omit the proof of this result, as it is a simplified version of the proof of the following Theorem 8.

9.2. Stokes problem

Firstly, observe that if each component of $\boldsymbol{u}$ satisfies Assumption 5, then from (97) we immediately get

$$\|h^{-1/2} \boldsymbol{R}_h^m \boldsymbol{u}\|_{0,\tilde{\Gamma}_h} \leq C_\infty\, h_\Gamma^{m+1/2}\, |\boldsymbol{u}|_{(W^{m+1,\infty}(\Omega_S))^n} . \tag{99}$$

This bound will be used in the proof of the following error estimate.

Theorem 8 (Enhanced L^2-error estimate for the velocity $\boldsymbol{u}_h$)**.** *Let each component of $\boldsymbol{u}$ satisfies Assumption 5, and let $p \in H^m(\Omega)$ and $\Gamma_N = \emptyset$. Under the conditions of validity of Theorem 2, the numerical velocity $\boldsymbol{u}_h$ produced by the SBM satisfies the following error estimate:*

$$\|\boldsymbol{u} - \boldsymbol{u}_h\|_{0,\tilde{\Omega}_h} \leq\; C\, l(\tilde{\Omega}_h)^{1/2} h_\Omega^{m+1/2} \left(|\boldsymbol{u}|_{m+1;\tilde{\Omega}_h} + h_\Omega^{1/2} |\boldsymbol{u}|_{(W^{m+1,\infty}(\Omega_S))^n} + |p|_{m;\tilde{\Omega}_h} \right) , \tag{100}$$

where C is a positive constant independent of the mesh size and the solution.

Proof. Given $z \in L^2(\tilde{\Omega}_h)^n$, let $\bar{z} \in L^2(\Omega)^n$ be its extension by $\boldsymbol{0}$ outside $\tilde{\Omega}_h$, and let $[\boldsymbol{\psi}, \lambda]$ be the solution of the following homogeneous Dirichlet problem in Ω:

$$-\nabla \cdot (2\,\mu\, \boldsymbol{\varepsilon}(\boldsymbol{\psi}) + \lambda \boldsymbol{I}) = \mu\, \bar{z} \qquad \text{in } \Omega\, , \tag{101a}$$

$$-\nabla \cdot \boldsymbol{\psi} = 0 \qquad \text{in } \Omega\, , \tag{101b}$$

$$\boldsymbol{\psi} = \boldsymbol{0} \qquad \text{on } \Gamma\, . \tag{101c}$$

The stated assumptions in addition to the fact that $\bar{z} \in L^2(\Omega)^n$ imply the regularity result $[\boldsymbol{\psi}, \lambda] \in (H^2(\Omega))^n \times H^1(\Omega)$, with the following bound

$$\|\mu^{1/2} \boldsymbol{\psi}\|_{2,\tilde{\Omega}_h} + \|\mu^{-1/2} \lambda\|_{1,\tilde{\Omega}_h} \leq\; \|\mu^{1/2} \boldsymbol{\psi}\|_{2,\Omega} + \|\mu^{-1/2} \lambda\|_{1,\Omega} \leq\; Q \|\mu^{1/2} \bar{z}\|_{0,\Omega} = Q \|\mu^{1/2} z\|_{0,\tilde{\Omega}_h} , \tag{102}$$

where $Q > 0$ is a non-dimensional constant independent of $\bar{z}$ and the mesh size.
The same arguments that led to (7) show that $\boldsymbol{\psi}$ satisfies on $\tilde{\Gamma}_h$

$$\boldsymbol{S}_h^1 \boldsymbol{\psi} + \boldsymbol{R}_h^1 \boldsymbol{\psi} = \boldsymbol{0}\, . \tag{103}$$

Thus, for any $[\boldsymbol{w}, q] \in \boldsymbol{W}(\tilde{\Omega}_h; \tilde{\mathscr{T}}_h)$ we have

$$\begin{aligned} \mu\, (z, \boldsymbol{w})_{0,\tilde{\Omega}_h} &= -(\nabla \cdot (2\,\mu\, \boldsymbol{\varepsilon}(\boldsymbol{\psi}) + \lambda \boldsymbol{I}), \boldsymbol{w})_{0,\tilde{\Omega}_h} - (\nabla \cdot \boldsymbol{\psi}, q)_{0,\tilde{\Omega}_h} \\ &= (2\,\mu\, \boldsymbol{\varepsilon}(\boldsymbol{\psi}), \boldsymbol{\varepsilon}(\boldsymbol{w}))_{0,\tilde{\Omega}_h} + (\lambda, \nabla \cdot \boldsymbol{w})_{0,\tilde{\Omega}_h} - (\nabla \cdot \boldsymbol{\psi}, q)_{0,\tilde{\Omega}_h} - (2\,\mu\, \boldsymbol{\varepsilon}(\boldsymbol{\psi}) + \lambda \boldsymbol{I}, \boldsymbol{w} \otimes \tilde{\boldsymbol{n}})_{0,\tilde{\Gamma}_h} \\ &= (2\,\mu\, \boldsymbol{\varepsilon}(\boldsymbol{\psi}), \boldsymbol{\varepsilon}(\boldsymbol{w}))_{0,\tilde{\Omega}_h} + (\lambda, \nabla \cdot \boldsymbol{w})_{0,\tilde{\Omega}_h} - (\nabla \cdot \boldsymbol{\psi}, q)_{0,\tilde{\Omega}_h} - (2\,\mu\, \boldsymbol{\varepsilon}(\boldsymbol{\psi}) + \lambda \boldsymbol{I}, \boldsymbol{S}_h^m \boldsymbol{w} \otimes \tilde{\boldsymbol{n}})_{0,\tilde{\Gamma}_h} \\ &\quad + \sum_{i=1}^m (2\,\mu\, \boldsymbol{\varepsilon}(\boldsymbol{\psi}) + \lambda \boldsymbol{I}, \frac{\mathscr{D}_{\boldsymbol{d}}^i \boldsymbol{w}}{i!} \otimes \tilde{\boldsymbol{n}})_{0,\tilde{\Gamma}_h} . \end{aligned} \tag{104}$$

Adding residual terms that vanish by definition when applied to the exact solution, we have

$$\begin{aligned} \mu(z, \boldsymbol{w})_{0,\tilde{\Omega}_h} = &\; (2\,\mu\, \boldsymbol{\varepsilon}(\boldsymbol{\psi}), \boldsymbol{\varepsilon}(\boldsymbol{w}))_{0,\tilde{\Omega}_h} + (\lambda, \nabla \cdot \boldsymbol{w})_{0,\tilde{\Omega}_h} - (\nabla \cdot \boldsymbol{\psi}, q)_{0,\tilde{\Omega}_h} - (2\,\mu\, \boldsymbol{\varepsilon}(\boldsymbol{\psi}) + \lambda \boldsymbol{I}, \boldsymbol{S}_h^m \boldsymbol{w} \otimes \tilde{\boldsymbol{n}})_{0,\tilde{\Gamma}_h} \\ &+ \sum_{i=1}^m (2\,\mu\, \boldsymbol{\varepsilon}(\boldsymbol{\psi}) + \lambda \boldsymbol{I}, \frac{\mathscr{D}_{\boldsymbol{d}}^i \boldsymbol{w}}{i!} \otimes \tilde{\boldsymbol{n}})_{0,\tilde{\Gamma}_h} - ((\boldsymbol{S}_h^1 \boldsymbol{\psi} + \boldsymbol{R}_h^1 \boldsymbol{\psi}) \otimes \tilde{\boldsymbol{n}}, 2\,\mu\, \boldsymbol{\varepsilon}(\boldsymbol{w}) - q \boldsymbol{I})_{0,\tilde{\Gamma}_h} + \gamma (2\,\mu\, h_\perp^{-1} (\boldsymbol{S}_h^1 \boldsymbol{\psi} + \boldsymbol{R}_h^1 \boldsymbol{\psi}), \boldsymbol{S}_h^m \boldsymbol{w})_{0,\tilde{\Gamma}_h} \end{aligned}$$

$$= \mathscr{B}_h([\boldsymbol{w},q];[\boldsymbol{\psi},\lambda]) - \delta \sum_{T\in\tilde{\mathscr{T}}_h} \left(h^2(2\mu)^{-1}\left(\nabla q - \nabla\cdot(2\,\mu\,\boldsymbol{\varepsilon}(\boldsymbol{w}))\right), \nabla\lambda\right)_{0,T} + \sum_{i=1}^{m}(2\,\mu\,\boldsymbol{\varepsilon}(\boldsymbol{\psi}) + \lambda \boldsymbol{I}, \frac{\mathscr{D}^i_{\boldsymbol{d}}\boldsymbol{w}}{i!}\otimes\tilde{\boldsymbol{n}})_{0,\tilde{\Gamma}_h}$$

$$- ((\nabla\boldsymbol{\psi}\,\boldsymbol{d})\otimes\tilde{\boldsymbol{n}}, 2\,\mu\,\boldsymbol{\varepsilon}(\boldsymbol{w}) - q\boldsymbol{I})_{0,\tilde{\Gamma}_h} - (\boldsymbol{R}^1_h\boldsymbol{\psi}\otimes\tilde{\boldsymbol{n}}, 2\,\mu\,\boldsymbol{\varepsilon}(\boldsymbol{w}) - q\boldsymbol{I})_{0,\tilde{\Gamma}_h} + \gamma\,(2\,\mu\,h_\perp^{-1}\boldsymbol{R}^1_h\boldsymbol{\psi}, \boldsymbol{S}^m_h\boldsymbol{w})_{0,\tilde{\Gamma}_h}\,. \tag{105}$$

Picking $\boldsymbol{w} = z = \boldsymbol{e_u} := \boldsymbol{u} - \boldsymbol{u}_h$, $q = e_p := p - p_h$, then $\mathscr{B}_h([\boldsymbol{w},q];[\boldsymbol{\psi},\lambda]) = \mathscr{B}_h([\boldsymbol{u},p];[\boldsymbol{\psi},\lambda]) - \mathscr{L}_h([\boldsymbol{\psi},\lambda])$. Thus, we can write the following identity, in which $[\boldsymbol{\psi}_I,\lambda_I] := [I^1_h\boldsymbol{\psi}, I^{SZ}_h\lambda]$:

$$\mu\|\boldsymbol{e_u}\|^2_{0,\tilde{\Omega}_h} = \mathscr{B}([\boldsymbol{e_u},e_p];[\boldsymbol{\psi}-\boldsymbol{\psi}_I,\lambda-\lambda_I]) + \mathscr{E}_{\mathrm{stab}}([\boldsymbol{e_u},e_p];[\boldsymbol{0},\lambda]) + \mathscr{E}_{\mathrm{sym}}([\boldsymbol{e_u},e_p];[\boldsymbol{\psi},\lambda])$$

$$+ \mathscr{E}_{\mathrm{rem}}([\boldsymbol{e_u},e_p];[\boldsymbol{\psi},\lambda]) + \mathscr{E}_{\mathrm{ort}}([\boldsymbol{u},p];[\boldsymbol{\psi}_I,\lambda_I])\,, \tag{106a}$$

with

$$\mathscr{E}_{\mathrm{stab}}([\boldsymbol{e_u},e_p];[\boldsymbol{0},\lambda]) := -\delta\sum_{T\in\tilde{\mathscr{T}}_h}\left(h^2(2\mu)^{-1}\left(\nabla e_p - \nabla\cdot(2\,\mu\,\boldsymbol{\varepsilon}(\boldsymbol{e_u}))\right), \nabla\lambda\right)_{0,T}\,, \tag{106b}$$

$$\mathscr{E}_{\mathrm{sym}}([\boldsymbol{e_u},e_p];[\boldsymbol{\psi},\lambda]) := \sum_{i=1}^{m}(2\,\mu\,\boldsymbol{\varepsilon}(\boldsymbol{\psi})\tilde{\boldsymbol{n}} + \lambda\tilde{\boldsymbol{n}}, \frac{\mathscr{D}^i_{\boldsymbol{d}}\boldsymbol{e_u}}{i!})_{0,\tilde{\Gamma}_h} - ((\nabla\boldsymbol{\psi}\,\boldsymbol{d})\otimes\tilde{\boldsymbol{n}}, 2\,\mu\,\boldsymbol{\varepsilon}(\boldsymbol{e_u}) - e_p\boldsymbol{I})_{0,\tilde{\Gamma}_h}\,, \tag{106c}$$

$$\mathscr{E}_{\mathrm{rem}}([\boldsymbol{e_u},e_p];[\boldsymbol{\psi},\lambda]) := -(\boldsymbol{R}^1_h\boldsymbol{\psi}\otimes\tilde{\boldsymbol{n}}, 2\,\mu\,\boldsymbol{\varepsilon}(\boldsymbol{e_u}) - e_p\boldsymbol{I})_{0,\tilde{\Gamma}_h} + \gamma\,\langle 2\,\mu\,h_\perp^{-1}\boldsymbol{R}^1_h\boldsymbol{\psi}, \boldsymbol{S}^m_h\boldsymbol{e_u}\rangle_{0,\tilde{\Gamma}_h}\,, \tag{106d}$$

$$\mathscr{E}_{\mathrm{ort}}([\boldsymbol{u},p];[\boldsymbol{\psi}_I,\lambda_I]) := (\boldsymbol{R}^m_h\boldsymbol{u}\otimes\tilde{\boldsymbol{n}}, 2\,\mu\,\boldsymbol{\varepsilon}(\boldsymbol{\psi}_I) + \lambda_I\boldsymbol{I})_{0,\tilde{\Gamma}_h} - \gamma\,(2\,\mu\,h^{-1}\boldsymbol{R}^m_h\boldsymbol{u}, \boldsymbol{S}^1_h\boldsymbol{\psi}_I)_{0,\tilde{\Gamma}_h}\,. \tag{106e}$$

We proceed to bound the error terms on the right-hand side of (106a). Recalling Theorem 4 and the analogue of Proposition 5 with $m = 1$ for $[\boldsymbol{\psi},\lambda]$, we have

$$|\mathscr{B}([\boldsymbol{e_u},e_p];[\boldsymbol{\psi}-\boldsymbol{\psi}_I,\lambda-\lambda_I])| \leq C_{\mathscr{B}}|||[\boldsymbol{e_u},e_p]|||_{\boldsymbol{W}(\tilde{\Omega}_h;\tilde{\mathscr{T}}_h)}|||[\boldsymbol{\psi}-\boldsymbol{\psi}_I,\lambda-\lambda_I]|||_{\boldsymbol{W}(\tilde{\Omega}_h;\tilde{\mathscr{T}}_h)}$$

$$\leq C_{\mathscr{B}}\,C_{APP}\,h_{\tilde{\Omega}_h}\left(\mu^{1/2}|\boldsymbol{\psi}|_{2,\tilde{\Omega}_h} + \mu^{-1/2}|\lambda|_{1,\tilde{\Omega}_h}\right)|||[\boldsymbol{e_u},e_p]|||_{\boldsymbol{W}(\tilde{\Omega}_h;\tilde{\mathscr{T}}_h)}$$

$$\lesssim h_{\tilde{\Omega}_h}\,\mu^{1/2}|||[\boldsymbol{e_u},e_p]|||_{\boldsymbol{W}(\tilde{\Omega}_h;\tilde{\mathscr{T}}_h)}\|\boldsymbol{e_u}\|_{0,\tilde{\Omega}_h}\,. \tag{107a}$$

From the definition of the norm $\boldsymbol{W}(\tilde{\Omega}_h;\tilde{\mathscr{T}}_h)$, writing $\boldsymbol{e_u} = (\boldsymbol{u} - I^m_h\boldsymbol{u}) + (I^m_h\boldsymbol{u} - \boldsymbol{u}_h)$, we get

$$|\mathscr{E}_{\mathrm{stab}}([\boldsymbol{e_u},e_p];[\boldsymbol{0},\lambda])| \leq \delta\,\|(2\,\mu)^{-1/2}h\,\nabla\lambda\|_{0,\tilde{\Omega}_h}\left(\|(2\,\mu)^{-1/2}h\,\nabla e_p\|_{0,\tilde{\Omega}_h} + \|(2\,\mu)^{1/2}h\,\nabla\cdot\boldsymbol{\varepsilon}(\boldsymbol{e_u})\|_{0,\tilde{\Omega}_h}\right)$$

$$\lesssim \left(\mu^{1/2}\,h_\Omega|||[\boldsymbol{e_u},e_p]|||_{\boldsymbol{W}(\tilde{\Omega}_h;\tilde{\mathscr{T}}_h)} + \mu^{1/2}h^{m+1}_\Omega|\boldsymbol{u}|_{m+1;\tilde{\Omega}_h}\right)\|\boldsymbol{e_u}\|_{0,\tilde{\Omega}_h}\,. \tag{107b}$$

Recalling the trace inequality $\|\nabla\boldsymbol{w}\|_{0,\tilde{\Gamma}_h} \leq c(\|\boldsymbol{w}\|_{1,\Omega} + |\nabla\boldsymbol{w}|_{1,\Omega})$, the bound $\sum_{i=1}^m\|h^{i-1/2}\mathscr{D}^i\boldsymbol{e_u}\|_{0,\tilde{\Gamma}_h} \leq C_D\|\boldsymbol{e_u}\|_{\boldsymbol{V}(\tilde{\Omega}_h;\tilde{\mathscr{T}}_h)}$ from Property 2, and the definition (68), we obtain, after using (5),

$$|\mathscr{E}_{\mathrm{sym}}([\boldsymbol{e_u},e_p];[\boldsymbol{\psi},\lambda])| \leq \sum_{i=1}^{m}\frac{\|h^{-1}\boldsymbol{d}\|^i_{L^\infty(\tilde{\Gamma}_h)}}{i!}\|(2\,\mu)^{1/2}h^{i-1/2}\mathscr{D}^i\boldsymbol{e_u}\|_{0,\tilde{\Gamma}_h}\left(\|(2\,\mu)^{1/2}h^{1/2}\boldsymbol{\varepsilon}(\boldsymbol{\psi})\|_{0,\tilde{\Gamma}_h} + \|(2\,\mu)^{-1/2}h^{1/2}\lambda\|_{0,\tilde{\Gamma}_h}\right)$$

$$+ \|h^{-1}\boldsymbol{d}\|_{L^\infty(\tilde{\Gamma}_h)}\|(2\,\mu)^{1/2}h^{1/2}\nabla\boldsymbol{\psi}\|_{0,\tilde{\Gamma}_h}\left(\|(2\,\mu)^{1/2}h^{1/2}\boldsymbol{\varepsilon}(\boldsymbol{e_u})\|_{0,\tilde{\Gamma}_h} + \|(2\,\mu)^{-1/2}h^{1/2}e_p\|_{0,\tilde{\Gamma}_h}\right)$$

$$\lesssim h^{1/2}_\Omega|||[\boldsymbol{e_u},e_p]|||_{\boldsymbol{W}(\tilde{\Omega}_h;\tilde{\mathscr{T}}_h)}\,l(\tilde{\Omega}_h)^{-3/2}\mu^{1/2}\|\boldsymbol{\psi}\|_{2,\tilde{\Omega}_h} + h^{1/2}_\Omega|||[\boldsymbol{e_u},e_p]|||_{\boldsymbol{W}(\tilde{\Omega}_h;\tilde{\mathscr{T}}_h)}l(\tilde{\Omega}_h)^{-1/2}\mu^{-1/2}\|\lambda\|_{1,\tilde{\Omega}_h}$$

$$\lesssim h^{1/2}_\Omega l(\tilde{\Omega}_h)^{1/2}\mu^{1/2}|||[\boldsymbol{e_u},e_p]|||_{\boldsymbol{W}(\tilde{\Omega}_h;\tilde{\mathscr{T}}_h)}\|\boldsymbol{e_u}\|_{0,\tilde{\Omega}_h}\,. \tag{107c}$$

On the other hand, applying Proposition 2 with $m = 1$ to each component of $\boldsymbol{\psi} \in (H^2(\Omega))^n$, we have

$$|\mathscr{E}_{\mathrm{rem}}([\boldsymbol{e_u},e_p];[\boldsymbol{\psi},\lambda])| \leq \left(\|(2\,\mu)^{1/2}h^{1/2}\boldsymbol{\varepsilon}(\boldsymbol{e_u})\|_{0,\tilde{\Gamma}_h} + \|(2\,\mu)^{-1/2}h^{1/2}e_p\|_{0,\tilde{\Gamma}_h}\right)\|(2\,\mu)^{1/2}h^{-1/2}\boldsymbol{R}^1_h\boldsymbol{\psi}\|_{0,\tilde{\Gamma}_h}$$

$$+ \gamma\|(2\,\mu)^{1/2}h^{-1/2}\boldsymbol{S}^1_h\boldsymbol{e_u}\|_{0,\tilde{\Gamma}_h}\|(2\,\mu)^{1/2}h^{-1/2}\boldsymbol{R}^1_h\boldsymbol{\psi}\|_{0,\tilde{\Gamma}_h}$$

$$+\gamma \sum_{i=2}^{m} \frac{\|h^{-1}\boldsymbol{d}\|^{i}_{L^\infty(\tilde{\Gamma}_h)}}{i!} \|(2\,\mu)^{1/2} h^{i-1/2} \mathscr{D}^i \boldsymbol{e_u}\|_{0,\tilde{\Gamma}_h} \|(2\,\mu)^{1/2} h^{-1/2} \boldsymbol{R}^1_h \boldsymbol{\psi}\|_{0,\tilde{\Gamma}_h}$$

$$\lesssim \mu^{1/2} |||[\boldsymbol{e_u}, e_p]|||_{W(\tilde{\Omega}_h;\tilde{\mathscr{T}}_h)} \|h^{-1/2}\boldsymbol{R}^1_h\boldsymbol{\psi}\|_{0,\tilde{\Gamma}_h} \lesssim h_\Omega\, \mu^{1/2} |||[\boldsymbol{e_u}, e_p]|||_{W(\tilde{\Omega}_h;\tilde{\mathscr{T}}_h)} \|\boldsymbol{e_u}\|_{0,\tilde{\Omega}_h} \,. \tag{107d}$$

At last, using once more the error estimates for the Scott-Zhang interpolant together with the identity (103) and the bound (99) of the remainder, we get

$$\begin{aligned}
|\mathscr{E}_{\rm ort}([\boldsymbol{u}, p]; [\boldsymbol{\psi}_I, \lambda_I])| = {}& |\langle \boldsymbol{R}^m_h \boldsymbol{u} \otimes \tilde{\boldsymbol{n}}, 2\,\mu\,\boldsymbol{\varepsilon}(\boldsymbol{\psi} - \boldsymbol{\psi}_I) + (\lambda - \lambda_I)\boldsymbol{I} - 2\,\mu\,\boldsymbol{\varepsilon}(\boldsymbol{\psi}) - \lambda \boldsymbol{I}\rangle_{0,\tilde{\Gamma}_h} \\
& + \gamma\,\langle 2\,\mu\, h^{-1} \boldsymbol{R}^m_h \boldsymbol{u}, \boldsymbol{S}^1_h(\boldsymbol{\psi} - \boldsymbol{\psi}_I) - \boldsymbol{S}^1_h \boldsymbol{\psi}\rangle_{0,\tilde{\Gamma}_h}| \\
\leq {}& \|(2\,\mu)^{1/2} h^{-1/2} \boldsymbol{R}^m_h \boldsymbol{u}\|_{0,\tilde{\Gamma}_h} \left(\|(2\,\mu)^{1/2} h^{1/2} \boldsymbol{\varepsilon}(\boldsymbol{\psi} - \boldsymbol{\psi}_I)\|_{0,\tilde{\Gamma}_h} + \|(2\,\mu)^{1/2} h^{1/2} \boldsymbol{\varepsilon}(\boldsymbol{\psi})\|_{0,\tilde{\Gamma}_h} \right) \\
& + \|(2\,\mu)^{1/2} h^{-1/2} \boldsymbol{R}^m_h \boldsymbol{u}\|_{0,\tilde{\Gamma}_h} \left(\|(2\,\mu)^{-1/2} h^{1/2} (\lambda - \lambda_I)\|_{0,\tilde{\Gamma}_h} + \|(2\,\mu)^{-1/2} h^{1/2} \lambda\|_{0,\tilde{\Gamma}_h} \right) \\
& + \gamma \|(2\,\mu)^{1/2} h^{-1/2} \boldsymbol{R}^m_h \boldsymbol{u}\|_{0,\tilde{\Gamma}_h} \left(\|(2\,\mu)^{1/2} h^{-1/2} \boldsymbol{S}^1_h (\boldsymbol{\psi} - \boldsymbol{\psi}_I)\|_{0,\tilde{\Gamma}_h} + \|(2\,\mu)^{1/2} h^{-1/2} \boldsymbol{R}^1_h \boldsymbol{\psi}\|_{0,\tilde{\Gamma}_h} \right) \\
\lesssim {}& h^{m+1}_\Omega\, l(\tilde{\Omega}_h)^{1/2} \mu\, \|\boldsymbol{e_u}\|_{0,\tilde{\Omega}_h} |\boldsymbol{u}|_{(W^{m+1,\infty}(\Omega_S))^n} \,.
\end{aligned} \tag{107e}$$

Thus, combining (107a), (107b), (107c), (107d), and (107e) in (106a) and applying Theorem 6 yields the desired result. □

Remark 12. *The previous bound is clearly sub-optimal due to the terms in* $\mathscr{E}_{\rm sym}([\boldsymbol{e_u}, e_p]; [\boldsymbol{\psi}, \lambda])$*. However, it is not clear at the moment if the above estimate is sharp, since in computations we always observe optimal, second-order convergence rates.*

10. Two-dimensional numerical tests

In this section, we perform convergence tests for the proposed high-order SBM approach for the Poisson and Stokes flow equations. All calculations were performed using the FEniCS software project [1].

Remark 13. *In all mesh refinement studies in this section, we do not apply Assumptions 2 or 3 to the definition of the distance* $\boldsymbol{d}$ *(for the Poisson and Stokes operators, respectively). Specifically the grids are refined by simply splitting every edge into two sub-edges at each stage of the mesh refinement procedure. While instrumental for the proofs of stability and convergence, Assumptions 2 or 3 may be too restrictive in practical engineering applications, and we prefer to forfeit them in the numerical tests, to show the overall robustness of the proposed methods under more general conditions.*

10.1. Poisson problem

In this first test, we considered Poisson's equation defined on a circular domain Ω of radius $r = 0.3$ centered at $[0.5, 0.5]$ as shown in Figure 3a. The exact solution is

$$u(x, y) = \sin(15\pi x)\sin(15\pi y)\,, \tag{108}$$

from which, using the method of manufactured solutions, the corresponding forcing f in (12) is deduced. Figure 3b depicts the surrogate domain on a coarse grid along with its surrogate boundary. Given $\kappa \in \{0.3, 1, 10\}$, we consider the Nitsche penalty parameter $\gamma = 2\,\kappa\, C_I\, \eta$ with η chosen as in equation 32, C_I chosen as in Property 3 and C_{inv} is the maximum eigenvalue of the problem:

Find $[\lambda_h, u_h], u_h \in \mathbb{P}_m(T)$, such that, $\forall v_h \in \mathbb{P}_m(T)$,

$$(\nabla(\nabla u_h), \nabla(\nabla v_h))_{0,T} - \lambda_h/h^2_T\, (\nabla u_h, \nabla v_h)_{0,T} = 0\,. \tag{109}$$

This approach is adopted from [33] and the results are given in Table 1 for a right isosceles triangular element (with vertices located at $(0,0)$, $(1,0)$ and $(0,1)$) and with $m = 2, 3, 4, 5$ and 6. In Figures 3c and 3d, we plot L^2-norm and

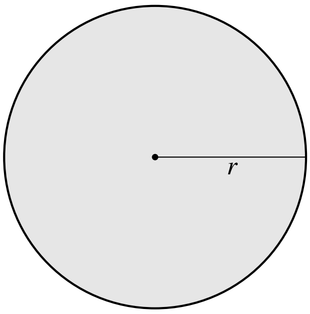

(a) The domain Ω (dark grey).

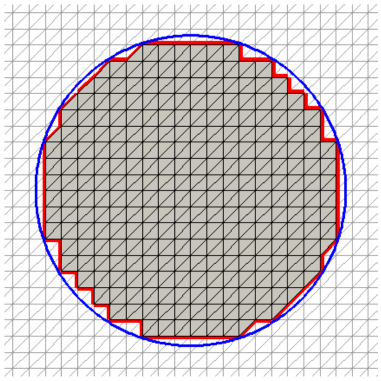

(b) $\tilde{\Omega}_h$ (grey), Γ (blue) and $\tilde{\Gamma}_h$ (red).

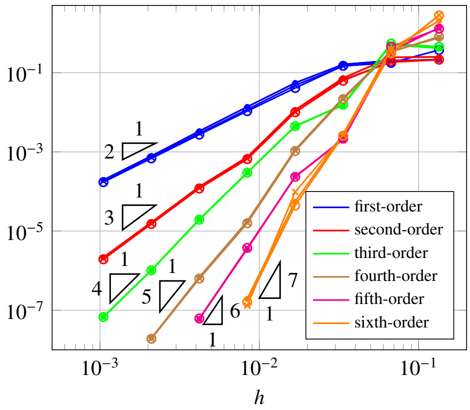

(c) Convergence rate of $\|u - u^h\|_{0,\tilde{\Omega}_h}$.

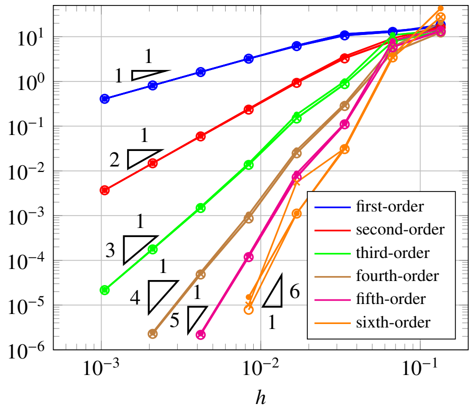

(d) Convergence rate of $|u - u^h|_{1,\tilde{\Omega}_h}$.

Figure 3: Poisson problem: The true domain Ω (top left), surrogate domain $\tilde{\Omega}_h$ (top right) and the $\|u - u^h\|_{0,\tilde{\Omega}_h}$ and $|u - u^h|_{1,\tilde{\Omega}_h}$ convergence rates using first, second, third, fourth, fifth and sixth order polynomials(bottom). The $\circ$, $\times$ and $\bullet$ markers refer to $\kappa = 0.3, 1,$ and 10, respectively.

H^1 semi-norm error rates for the SBM using first, second, third, fourth, fifth and sixth order polynomials respectively. The L^2-norm and H^1-semi-norm errors converge optimally under all polynomial orders regardless of the choice of κ. In particular, the L^2-norm converges faster than the predicted theoretical rate of $m + 1/2$.

mth-order polynomial	C_{inv}
2	36.00
3	155.05
4	397.50
5	848.10
6	1591.60[a]

Table 1: Values of the constant C_{inv} for right isosceles triangles. [a] Calculated by extrapolating a cubic polynomial calibrated with the C_{inv} values of $m = 2, 3, 4$ and 5

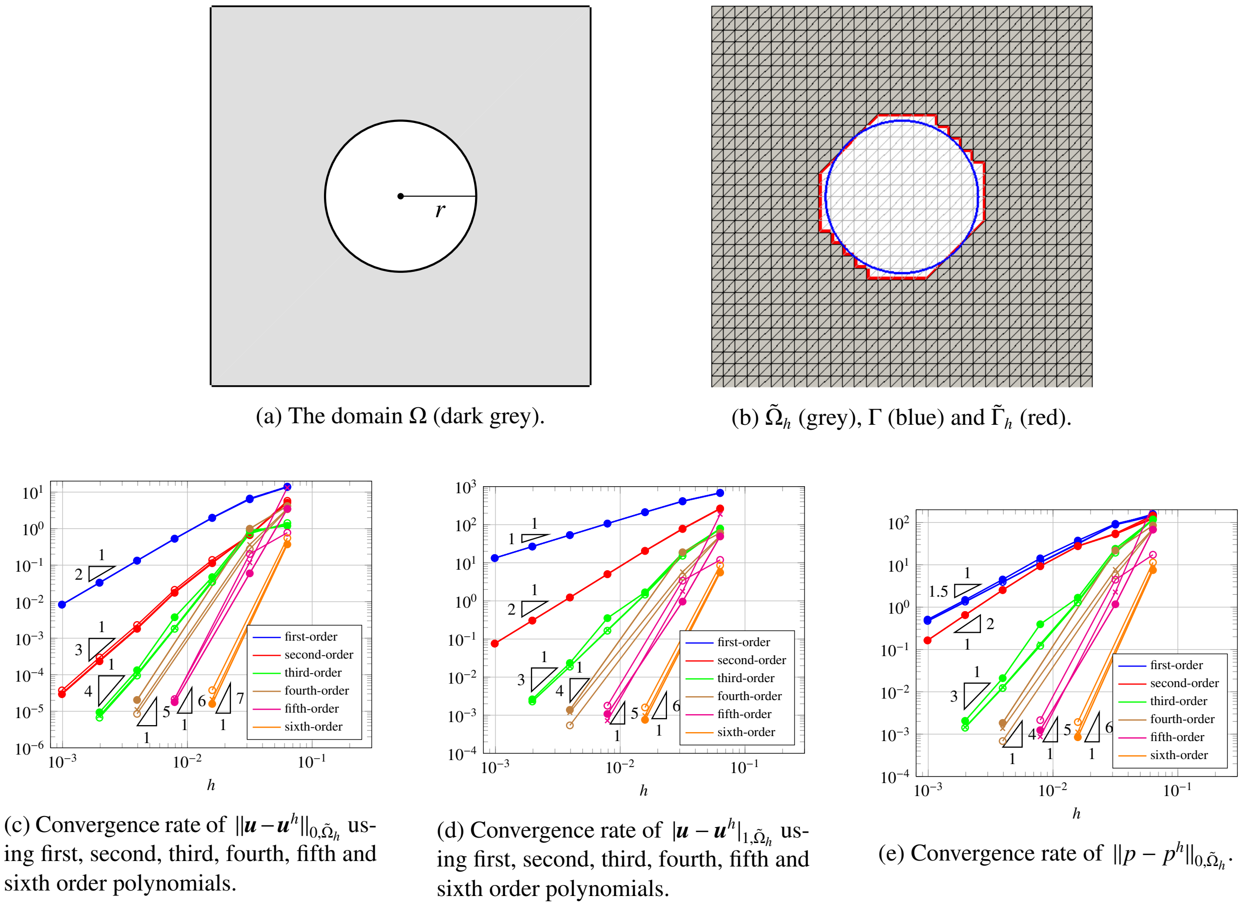

(a) The domain Ω (dark grey).

(b) $\tilde{\Omega}_h$ (grey), Γ (blue) and $\tilde{\Gamma}_h$ (red).

(c) Convergence rate of $\|\boldsymbol{u} - \boldsymbol{u}^h\|_{0,\tilde{\Omega}_h}$ using first, second, third, fourth, fifth and sixth order polynomials.

(d) Convergence rate of $|\boldsymbol{u} - \boldsymbol{u}^h|_{1,\tilde{\Omega}_h}$ using first, second, third, fourth, fifth and sixth order polynomials.

(e) Convergence rate of $\|p - p^h\|_{0,\tilde{\Omega}_h}$.

Figure 4: Stokes problem: The true domain Ω (top left), surrogate domain $\tilde{\Omega}_h$ (top right) and the $\|\boldsymbol{u} - \boldsymbol{u}^h\|_{0,\tilde{\Omega}_h}$, $|\boldsymbol{u} - \boldsymbol{u}^h|_{1,\tilde{\Omega}_h}$ and $\|p - p^h\|_{0,\tilde{\Omega}_h}$ convergence rates using first, second, third, fourth, fifth and sixth order polynomials (bottom).The $\circ$, $\times$ and $\bullet$ markers refer to $\kappa = 0.3, 1,$ and 10, respectively.

10.2. *Stokes flow problem*

In this test, we consider Stokes flow equations on a unit square domain with circular hole of radius $r = 0.2$ centered at $[0.5, 0.5]$ denoted by Ω as shown in Figure 4a. We adopt the exact solution in [6] given as

$$\begin{cases} p(x,y) = \cos(10\pi x)\cos(10\pi y) - 1 \ , \\ u_x(x,y) = 10\pi \sin(10\pi x)\sin(10\pi y) \ , \\ u_y(x,y) = 10\pi \cos(10\pi x)\cos(10\pi y) \ . \end{cases} \tag{110}$$

with a fluid viscosity μ set equal to 1. Figure 4b depicts the surrogate domain on a coarse grid along with its surrogate boundary. Dirichlet conditions are enforced with the SBM on the circular hole while body-fitted Dirichlet conditions are weakly enforced on the top and bottom boundaries and traction conditions are applied at the left and right boundaries. Given $\kappa \in \{0.3, 1, 10\}$, we consider the Nitsche penalty parameter $\gamma = 2\,\kappa\, C_I\, \eta$ and the pressure stabilization parameter $\delta = 0.6 C_{inv}^{-1}$ with η chosen as in equation 51, C_I chosen similarly to Section 10.1 and C_{inv} is given in Table 1.

The convergence tests were conducted using first, second, third, fourth, fifth and sixth order polynomials. The L^2-norm and H^1-seminorm of the velocity errors are reported in Figures 4c and 4d respectively, while in Figure 4e we plot the L^2-norm pressure errors. Both L^2-norm and H^1-seminorm errors converge optimally under all polynomial orders. In particular, the L^2-norm errors on the velocity exceed the theoretical estimate of $m+1/2$ derived in Section 9.

11. Summary

We have presented the high-order version of the SBM, in the case of the Poisson and Stokes operators. We provided a complete mathematical analysis of stability and convergence in the natural norm of the SBM, as well as L^2-error estimates. We have confirmed with a number of numerical experiments the results of the numerical analysis. Similarly to the low-order version of the SBM, we observed that, despite a suboptimal L^2-error estimate, the L^2 norm of the error converges optimally in the numerical tests.

Acknowledgments

The support of the Army Research Office (ARO) under Grant W911NF-18-1-0308 and Lawrence Livermore National Laboratory under an LDRD grant is gratefully acknowledged. The computations were performed on a computer cluster sponsored by the Army Office of Research under grant W911NF-15-1-0382.

CC performed this research in the framework of the Italian MIUR Award "Dipartimenti di Eccellenza 2018-2022" granted to the Department of Mathematical Sciences, Politecnico di Torino (CUP: E11G18000350001), and with the support of the Italian MIUR PRIN Project 201752HKH8-003. He is a member of the Italian INdAM-GNCS research group.

References

[1] Martin S. Alnæs, Jan Blechta, Johan Hake, August Johansson, Benjamin Kehlet, Anders Logg, Chris Richardson, Johannes Ring, Marie E. Rognes, and Garth N. Wells. The fenics project version 1.5. Archive of Numerical Software, 3(100), 2015.

[2] N. M. Atallah, C. Canuto, and G. Scovazzi. Analysis of the Shifted Boundary Method for the Poisson problem in domains with corners. Math. Comp., 90:2041–2069, 2021.

[3] Nabil M. Atallah, Claudio Canuto, and Guglielmo Scovazzi. Analysis of the shifted boundary method for the stokes problem. Computer Methods in Applied Mechanics and Engineering, 358:112609, 2020.

[4] Nabil M. Atallah, Claudio Canuto, and Guglielmo Scovazzi. The second-generation Shifted Boundary Method and its numerical analysis. Computer Methods in Applied Mechanics and Engineering, 372:113341, 2020.

[5] Nabil M. Atallah, Claudio Canuto, and Guglielmo Scovazzi. The shifted boundary method for solid mechanics. International Journal for Numerical Methods in Engineering, https://doi.org/10.1002/nme.6779, 2021.

[6] Santiago Badia and Ramon Codina. Unified stabilized finite element formulations for the Stokes and the Darcy problems. SIAM journal on Numerical Analysis, 47(3):1971–2000, 2009.

[7] Peter Bastian and Christian Engwer. An unfitted finite element method using discontinuous galerkin. International journal for numerical methods in engineering, 79(12):1557–1576, 2009.

[8] Yuri Bazilevs, Victor M Calo, John A Cottrell, John A Evans, Thomas Jr R Hughes, S Lipton, Michael A Scott, and Thomas W Sederberg. Isogeometric analysis using t-splines. Computer Methods in Applied Mechanics and Engineering, 199(5):229 – 263, 2010.

[9] D. Boffi and L. Gastaldi. A finite element approach for the immersed boundary method. Comput. Struct., 81(8):491–501, 2003.

[10] Thomas Boiveau and Erik Burman. A penalty-free Nitsche method for the weak imposition of boundary conditions in compressible and incompressible elasticity. IMA Journal of Numerical Analysis, 36, 07 2014.

[11] Thomas Boiveau, Erik Burman, Susanne Claus, and Mats Larson. Fictitious domain method with boundary value correction using penalty-free nitsche method. Journal of Numerical Mathematics, 26(2):77–95, 2018.

[12] J. Bramble and J. King. A robust finite element method for nonhomogeneous Dirichlet problems in domains with curved boundaries. Math. Comp., 63:1–17, 1994.

[13] J. H. Bramble, T. Dupont, and V. Thomée. Projection methods for Dirichlet's problem in approximating polygonal domains with boundary-value corrections. Math. Comp., 26:869–879, 1972.

[14] E. Burman. Ghost penalty. C. R. Math., 348(21-22):1217–1220, 2010.

[15] E. Burman, S. Claus, P. Hansbo, M. G. Larson, and A. Massing. CutFEM: Discretizing geometry and partial differential equations. Int. J. Numer. Methods Eng., 104(7):472–501, 2015.

[16] E. Burman, P. Hansbo, and M. Larson. A cut finite element method with boundary value correction. Math. Comp., 87(310):633–657, 2018.

[17] E. Burman, P. Hansbo, and M. G. Larson. A cut finite element method with boundary value correction for the incompressible Stokes equations. In European Conference on Numerical Mathematics and Advanced Applications, pages 183–192. Springer, 2017.

[18] Erik Burman. Ghost penalty. Comptes Rendus Mathematique, 348(21):1217–1220, November 2010.

[19] Erik Burman, Matteo Cicuttin, Guillaume Delay, and Alexandre Ern. An unfitted hybrid high-order method with cell agglomeration for elliptic interface problems. SIAM Journal on Scientific Computing, 43(2):A859–A882, 2021.

[20] Erik Burman and Peter Hansbo. Fictitious domain methods using cut elements: Iii. a stabilized Nitsche method for Stokes' problem. ESAIM: Mathematical Modelling and Numerical Analysis, 48(3):859–874, 2014.

[21] Erik Burman, Peter Hansbo, and Mats G Larson. Dirichlet boundary value correction using lagrange multipliers. BIT Numerical Mathematics, 60(1):235–260, 2020.

[22] Erik Burman, Cuiyu He, and Mats G Larson. A posteriori error estimates with boundary correction for a cut finite element method. arXiv preprint arXiv:1906.00879, 2019.

[23] James Cheung, Max Gunzburger, Pavel Bochev, and Mauro Perego. An optimally convergent higher-order finite element coupling method for interface and domain decomposition problems. Results in Applied Mathematics, 6:100094, 2020.

[24] B. Cockburn, D. Gupta, and F. Reitich. Boundary-conforming discontinuous Galerkin methods via extensions from subdomains. J Sci Comput., 42:144, 2010.

[25] B. Cockburn and M. Solano. Solving Dirichlet boundary-value problems on curved domains by extensions from subdomains. SIAM J. Sci. Comput., 34(1):A497–A519, 2012.

[26] Bernardo Cockburn, Weifeng Qiu, and Manuel Solano. A priori error analysis for HDG methods using extensions from subdomains to achieve boundary conformity. Math. Comp., 83:665–699, 03 2014.

[27] J Austin Cottrell, Alessandro Reali, Yuri Bazilevs, and Thomas JR" Hughes. Isogeometric analysis of structural vibrations. Computer Methods in Applied Mechanics and Engineering, 195(41):5257–5296, 2006.

[28] Alexander Düster, Jamshid Parvizian, Zhengxiong Yang, and Ernst Rank. The finite cell method for three-dimensional problems of solid mechanics. Comput. Methods Appl. Mech. Eng., 197(45):3768–3782, 2008.

[29] P. Grisvard. Elliptic problems in nonsmooth domains. Classics in Applied Mathematics. Society for Industrial and Applied Mathematics (SIAM), Philadelphia, PA, 2011.

[30] A. Hansbo and P. Hansbo. An unfitted finite element method, based on Nitsche's method, for elliptic interface problems. Comput. Methods Appl. Mech. Eng., 191(47):5537–5552, 2002.

[31] Anita Hansbo and Peter Hansbo. An unfitted finite element method, based on nitsche's method, for elliptic interface problems. Computer Methods in Applied Mechanics and Engineering, 191(47):5537 – 5552, 2002.

[32] Peter Hansbo, Mats G Larson, and Karl Larsson. Cut finite element methods for linear elasticity problems. In Geometrically unfitted finite element methods and applications, pages 25–63. Springer, 2017.

[33] Isaac Harari and Thomas J.R. Hughes. What are C and h?: Inequalities for the analysis and design of finite element methods. Comput. Methods Appl. Mech. Eng., 97(2):157–192, 1992.

[34] K. Höllig. Finite element methods with B-splines. SIAM, 2003.

[35] Thomas J. R. Hughes and Leopoldo P. Franca. A new finite element formulation for computational fluid dynamics: VII. The Stokes problem with various well-posed boundary conditions: Symmetric formulations that converge for all velocity/pressure spaces. Comput. Methods Appl. Mech. Eng., 65(1):85 – 96, 1987.

[36] D. Kamensky, MC. Hsu, Y. Yu, J. A. Evans, M. S. Sacks, and T. J. R. Hughes. Immersogeometric cardiovascular fluid–structure interaction analysis with divergence-conforming b-splines. Comput. Methods Appl. Mech. Eng., 314:408–472, 2017.

[37] E. N. Karatzas, G. Stabile, N. Atallah, G. Scovazzi, and G. Rozza. A reduced order approach for the embedded shifted boundary fem and a heat exchange system on parametrized geometries. In IUTAM Symposium on Model Order Reduction of Coupled Systems, Stuttgart, Germany, May 22–25, 2018, pages 111–125. Springer, 2020.

[38] E. N. Karatzas, G. Stabile, L. Nouveau, G. Scovazzi, and G. Rozza. A reduced basis approach for pdes on parametrized geometries based on the shifted boundary finite element method and application to a Stokes flow. Comput. Methods Appl. Mech. Eng., 347:568–587, 2019.

[39] E. N. Karatzas, G. Stabile, L. Nouveau, G. Scovazzi, and G. Rozza. A reduced-order Shifted Boundary Method for parametrized incompressible Navier-Stokes equations. arXiv preprint arXiv:1907.10549, 2019.

[40] Christoph Lehrenfeld. High order unfitted finite element methods on level set domains using isoparametric mappings. Computer Methods in Applied Mechanics and Engineering, 300:716–733, 2016.

[41] Christoph Lehrenfeld and Arnold Reusken. Analysis of a high-order unfitted finite element method for elliptic interface problems. IMA Journal of Numerical Analysis, 38(3):1351–1387, 2018.

[42] A. Main and G. Scovazzi. The Shifted Boundary Method for embedded domain computations. Part i: Poisson and Stokes problems. J. Comput. Phys., 372:972–995, 2018.

[43] A. Main and G. Scovazzi. The Shifted Boundary Method for embedded domain computations. Part ii: Linear advection–diffusion and incompressible Navier–Stokes equations. J. Comput. Phys., 372:996–1026, 2018.

[44] Nicolas Moës, John Dolbow, and Ted Belytschko. A finite element method for crack growth without remeshing. International journal for numerical methods in engineering, 46(1):131–150, 1999.

[45] J. Nitsche. Uber ein variationsprinzip zur losung dirichlet-problemen bei verwendung von teilraumen, die keinen randbedingungen unteworfen sind. Abhandlungen aus dem Mathematischen Seminar der Universitat Hamburg, 36(1):9–15, July 1971.

[46] J. Nitsche. Über ein Variationsprinzip zur Lösung von Dirichlet-problemen bei Verwendung von Teilräumen. Abh. Math. Semin. Univ. Hambg., 36:9–15, 1971.

[47] Maxim A Olshanskii and Danil Safin. Numerical integration over implicitly defined domains for higher order unfitted finite element methods. Lobachevskii Journal of Mathematics, 37(5):582–596, 2016.

[48] Ricardo Oyarzúa, Manuel Solano, and Paulo Zúñiga. A high order mixed-FEM for diffusion problems on curved domains. J. Sci. Comput., 79(1):49–78, 2019.

[49] Ricardo Oyarzúa, Manuel Solano, and Paulo Zúñiga. A priori and a posteriori error analyses of a high order unfitted mixed-fem for stokes flow. Computer Methods in Applied Mechanics and Engineering, 360:112780, 2020.

[50] J. Parvizian, A. Düster, and E. Rank. Finite cell method. Comput. Mech, 41(1):121–133, 2007.

[51] C. S. Peskin. Flow patterns around heart valves: a numerical method. J. Comput. Phys., 10(2):252–271, 1972.

[52] Janosch Preuß. Higher order unfitted isoparametric space-time fem on moving domains. Master's thesis, University of Gottingen, 2018.

[53] Ramsharan Rangarajan and Adrian J Lew. Universal meshes: A new paradigm for computing with nonconforming triangulations. arXiv preprint arXiv:1201.4903, 2012.

[54] Ramsharan Rangarajan and Adrian J Lew. Analysis of a method to parameterize planar curves immersed in triangulations. SIAM Journal on Numerical Analysis, 51(3):1392–1420, 2013.

[55] Ramsharan Rangarajan and Adrián J Lew. Universal meshes: A method for triangulating planar curved domains immersed in nonconforming meshes. International Journal for Numerical Methods in Engineering, 98(4):236–264, 2014.

[56] T. Rüberg and F. Cirak. Subdivision-stabilised immersed b-spline finite elements for moving boundary flows. Comput. Methods Appl. Mech.

Eng., 209:266–283, 2012.
[57] Dominik Schillinger, Luca Dede, Michael A Scott, John A Evans, Michael J Borden, Ernst Rank, and Thomas JR Hughes. An isogeometric design-through-analysis methodology based on adaptive hierarchical refinement of nurbs, immersed boundary methods, and t-spline cad surfaces. Computer Methods in Applied Mechanics and Engineering, 249–252:116 – 150, 2012.
[58] B. Schott, U. Rasthofer, V. Gravemeier, and W. A. Wall. A face-oriented stabilized nitsche-type extended variational multiscale method for incompressible two-phase flow. International Journal for Numerical Methods in Engineering, 104(7):721–748, 2015.
[59] B Schott and WA Wall. A new face-oriented stabilized xfem approach for 2d and 3d incompressible navier–stokes equations. Computer Methods in Applied Mechanics and Engineering, 276:233–265, 2014.
[60] T. Song, A. Main, G. Scovazzi, and M. Ricchiuto. The Shifted Boundary Method for hyperbolic systems: Embedded domain computations of linear waves and shallow water flows. J. Comput. Phys., 369:45–79, 2018.
[61] T. Warburton and J.S. Hesthaven. On the constants in hp-finite element trace inverse inequalities. Computer Methods in Applied Mechanics and Engineering, 192(25):2765–2773, 2003.

Appendix: some useful inequalities

We recall some useful scaled trace inequalities and inverse inequalities in shape-regular triangulations.

Property 3. *There exists a constant $C_I > 0$ independent of the meshsize such that for any $T \in \tilde{\mathscr{T}}_h$ and any edge/face $E \subset \partial T$ it holds*

$$\|h_T^{1/2} w\|^2_{0,E} \leq C_I \, \|w\|^2_{0,T} \,, \qquad \forall w \in \mathbb{P}_k(T) \,, \qquad 1 \leq k \leq m \,. \tag{111}$$

This immediately gives

$$\|h^{1/2} \partial^i v_h\|^2_{0,\tilde{\Gamma}_h} \leq C_I \, \|\partial^i v_h\|^2_{0,\tilde{\Omega}_h} \,, \qquad \forall v_h \in V_h \,, \qquad 0 \leq i \leq m \,, \tag{112}$$

where $\partial^i v_h$ denotes any partial derivative of order i of v_h. From [61], we estimate

$$C_I = \begin{cases} (k+1-i)\,(k+n-i)\,n^{-1} & \textit{for simplices in n dimensions} \\ (k+1-i)^2 & \textit{for quadrilaterals and hexahedra.} \end{cases} \tag{113}$$

Property 4. *There exists a constant $C_{inv} > 0$ independent of the meshsize such that for any $T \in \tilde{\mathscr{T}}_h$ it holds*

$$|w|^2_{i,T} \leq C_{inv} \, h_T^{2(1-i)} \, \|\nabla w\|^2_{0,T} \,, \qquad \forall w \in \mathbb{P}_m(T) \,, \qquad 1 \leq i \leq m, \tag{114}$$

where $|w|_{i,T}$ denotes the Sobolev semi-norm of w in T.

Corollary 1. *For any $T \in \tilde{\mathscr{T}}_h$ and any edge/face $E \subset \partial T$ it holds*

$$\|h_T^{-1/2} \mathscr{D}^i_{\boldsymbol{d}} \, w\|_{0,E} \leq C_I^{1/2} C_{inv}^{1/2} \|h_T^{-1} \boldsymbol{d}\|^i_{L^\infty(E)} \|\nabla w\|_{0,T} \,, \qquad \forall w \in \mathbb{P}_m(T) \,, \qquad 1 \leq i \leq m \,. \tag{115}$$

This immediately gives

$$\|h^{-1/2} \mathscr{D}^i_{\boldsymbol{d}} \, v_h\|_{0,\tilde{\Gamma}_h} \leq C_I^{1/2} C_{inv}^{1/2} \|h^{-1} \boldsymbol{d}\|^i_{L^\infty(\tilde{\Gamma}_h)} \|\nabla v_h\|_{0,\tilde{\Omega}_h} \,, \qquad \forall v_h \in V_h \,, \qquad 1 \leq i \leq m \,. \tag{116}$$

Proof. Writing $\boldsymbol{d} = \|\boldsymbol{d}\| \, \boldsymbol{\nu}$, one has $\mathscr{D}^i_{\boldsymbol{d}} \, w = \|\boldsymbol{d}\|^i \mathscr{D}^i_{\boldsymbol{\nu}} \, w$ with $|\mathscr{D}^i_{\boldsymbol{\nu}} \, w| \leq \|\boldsymbol{D}^i w\|$. From Properties 3 and 4,

$$\|h_T^{-1/2} \mathscr{D}^i_{\boldsymbol{d}} \, w\|_{0,E} \quad \leq \quad \|\boldsymbol{d}\|^i_{L^\infty(E)} \|h_T^{-1/2} \boldsymbol{D}^i w\|_{0,E} \leq C_I^{1/2} h_T^{-1} \|\boldsymbol{d}\|^i_{L^\infty(E)} \|\boldsymbol{D}^i w\|_{0,T} \leq C_I^{1/2} C_{inv}^{1/2} \|h_T^{-1} \boldsymbol{d}\|^i_{L^\infty(E)} \|\nabla w\|_{0,T} \,,$$

which concludes the proof. □

Finally, we recall the following inequality of the Korn type for H^1-vector fields, which can be found in [10].

Theorem 9 (Korn's inequality). *Let $\tilde{\Omega}_h$ be a domain in $\mathbb{R}^n$ with $n \geq 2$, and let $\tilde{\Gamma}_h \subseteq \partial\tilde{\Omega}_h$ have positive $(n-1)$-dimensional measure. Then, there exists a constant $\bar{C}_K > 0$ such that for all $\boldsymbol{u} \in (H^1(\tilde{\Omega}_h))^n$ it holds*

$$\|\boldsymbol{u}\|^2_{H^1(\tilde{\Omega}_h)} \leq \bar{C}_K \left(l(\tilde{\Omega}_h)^{-1} \|\boldsymbol{u}\|^2_{0,\tilde{\Gamma}_h} + \|\boldsymbol{\varepsilon}(\boldsymbol{u})\|^2_{0,\tilde{\Omega}_h} \right) \,. \tag{117}$$